Applied Thermal Engineering 236 (2024) 121743

Contents lists available at ScienceDirect

Applied Thermal Engineering

journal homepage: www.elsevier.com/locate/ate

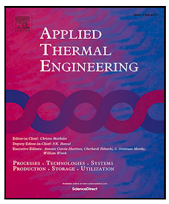

Research Paper

Development of map-based models for the performance characterization in a new prototype of Dual Source Heat Pump

Javier Marchante-Avellaneda [a,*], Emilio Navarro-Peris [a], Yang Song [b]

[a] Instituto Universitario de Investigación en Ingeniería Energética, Universitat Politècnica de València, Camino de Vera s/n, 46022 Valencia, Spain
[b] Department of Energy Technology, Division of Applied Thermodynamics and Refrigeration, Royal Institute of Technology, SE-100 44 Stockholm, Sweden

ARTICLE INFO

Keywords:
Polynomial models
Heat pump performance
Ground source heat pump
Air source heat pump
Dual source heat pump

ABSTRACT

This paper presents the development of accurate map-based models for characterizing a new Dual Source Heat Pump prototype. This unit includes three braze plate heat exchangers and a round tube fin heat exchanger, allowing the unit to select different operating modes such as heat pump, chiller, and domestic hot water production using as source the ground or air. Therefore, due to the hybrid typology of this unit and the possibility of reversing the cycle, this work covers the main heat pump and refrigeration equipment technologies currently available on the market (air source and ground source units). The modeling strategy selected has been to provide several polynomial expressions to predict the performance of these units, i.e., compressor energy consumption and condenser and evaporator capacities. This approach allows obtaining accurate, compact, and easy-to-implement models for developing dynamic models of more complex systems where this type of unit – the heat pump – is an integrated part of the system. Currently, a clear example of this modeling strategy can be found in characterizing one of the main components installed in these machines, the compressor. The AHRI-540 standard specifies a polynomial model as a function of evaporating and condensing temperatures. In this sense, for the characterization of heat pumps, the polynomials developed depend only on the unit's external variables, so they can be useful in many scenarios, obtaining direct feedback on the heat pump performance when developing a dynamic model to optimize system control strategies or to develop techno-economic studies. In this case, the hybrid typology of this unit makes it particularly relevant to optimize the control to manage the type of source to be used (air or ground), allowing the development of a more efficient and sustainable technology by selecting the most adequate source in terms of performance. This study focuses on obtaining the polynomial expressions that minimize the number of terms while simultaneously minimizing prediction error. By carefully selecting the most significant terms and suitable transformations in the characterized variables, the goal is to prevent overfitting, minimize potential extrapolation or interpolation errors and obtain polynomial expressions that can be fitted with small experimental samples. For this purpose, a detailed model implemented in a commercial software for heat pump characterization has been used, with which a large number of simulation results were generated. These simulation results include a fine meshing working map of the unit that allowed us to analyze the relationships between the characterized and external variables.

1. Introduction

The modeling of heat pumps and refrigeration equipment can be beneficial when analyzing more complex systems where such units are integrated. In recent years, the ability to model their behavior has become even more relevant with the current growth of new cooling and heating technologies with variable speed components, where the design and analysis of suitable control strategies is essential in order to cover the user demand by maintaining a high working efficiency of the unit. In this sense, characteristics of a desirable model are simplicity and dependence on parameters that can easily define an average user and be monitored in real installations. Hamilton [1] presented a classification for air conditioning equipment models, differentiating between *"equation-fit"* models (empirical models) and *"deterministic"* models (theoretical models). Therefore, heat pump models also can be generally classified in terms of the degree of complexity and empiricism. Some of them can provide simple correlations as black-box models to directly predict heat pump performance ($\dot{Q}_c$, $\dot{Q}_e$, $\dot{W}_c$) in steady-state conditions. Other models can develop a more detailed

* Corresponding author.
E-mail addresses: jamarav@iie.upv.es (J. Marchante-Avellaneda), emilio.navarro@iie.upv.es (E. Navarro-Peris), yson@kth.se (Y. Song).

https://doi.org/10.1016/j.applthermaleng.2023.121743
Received 12 July 2023; Received in revised form 8 September 2023; Accepted 3 October 2023
Available online 6 October 2023

Nomenclature

Acronyms

AIC	Akaike Information Criterion
ccp	Correlation coefficient of Pearson
CV_{RMSE}	Coefficient of Variation of the RMSE
DHWA	Domestic Hot Water Air operating mode
DHWG	Domestic Hot Water Ground operating mode
DHWU	Domestic Hot Water User operating mode
DSHP	Dual Source Heat Pump
MRE	Maximum Relative Error (%)
pccp	Partial correlation coefficient of Pearson
RH	Relative Humidity (%)
RMSE	Root Mean Square Error (W)
SA	Summer Air operating mode
SG	Summer Ground operating mode
WA	Winter Air operating mode
WG	Winter Ground operating mode

Symbols

dT_c	Temperature difference of the secondary fluid across the condenser (K)
dT_e	Temperature difference of the secondary fluid across the evaporator (K)
f_c	Compressor frequency (Hz)
f_{fan}	Fan speed (%)
$\dot{m}_{ref}$	Refrigerant mass flow rate (kg/s)
n	Compressor speed (rps)
P_{atm}	Atmospheric pressure. 1.013 (bar)
P_e	Evaporation pressure (bar)
$P_{h,user}$	Circulation pump hydraulic power, user loop (W)
$P_{h,ground}$	Circulation pump hydraulic power, ground loop (W)
$\dot{Q}_c$	Condenser capacity (W)
$\dot{Q}_{cooling}$	Cooling capacity (W)
$\dot{Q}_e$	Evaporator capacity (W)
$\dot{Q}_{heating}$	Heating capacity
RH	Relative humidity (%)
T_{ai}	Air inlet temp. to the RTPFHx (°C or K)
T_c	Dew point condensation temperature (°C)
T_{ci}	Inlet temperature of the secondary fluid to the condenser (°C or K)
T_{co}	Outlet temperature of the secondary fluid to the condenser (°C or K)
T_e	Dew point evaporation temperature (°C)
T_{ei}	Inlet temperature of the secondary fluid to the evaporator (°C or K)
T_{eo}	Outlet temperature of the secondary fluid to the evaporator (°C or K)
V_s	Compressor swept volume (m^3)
w_{ai}	Humidity ratio at RTPFHx inlet conditions ($kg_{water}/kg_{dry\ air}$)
$\dot{W}_c$	Compressor energy consumption (W)
$\dot{W}_{DSHP}$	DSHP energy consumption (W)
$\dot{W}_{fan}$	Fan energy consumption (W)
$\dot{W}_{ground,pump}$	Circulation pump energy consumption, ground loop (W)
$\dot{W}_{par}$	Parasitic consumption (W)
w_{sat}	Humidity ratio at saturated conditions ($kg_{water}/kg_{dry\ air}$)
$\dot{W}_{user,pump}$	Circulation pump energy consumption, user loop (W)
Δw	$w_{ai} - w_{sat}$ ($kg_{water}/kg_{dry\ air}$)
$\Delta w'$	$\max[w_{ai} - w_{sat}, 0]$ ($kg_{water}/kg_{dry\ air}$)
δT_e	Difference temperature between primary and secondary loop in the evaporator (temperature approach) (K)
η_c	Compressor efficiency (%)
η_p	Circulation pump motor efficiency (%)
η_v	Volumetric efficiency (%)
ξ	Compressor heat losses (%)
ρ_s	Refrigerant density at compressor suction conditions (kg/m^3)

definition, modeling its components. In past years, some detailed simulation tools have assisted heat pump manufacturers. Some examples of these simulation tools are the ORNL Heat Pump Design Model [2], the CYCLE_D-HX software [3], the VapCyc and Coil Designer software [4–6], or the simulation tool IMST-ART [7,8], where the heat pump unit is implemented by defining its individual components (commonly with the data extracted from the manufacturer's catalog). However, the main problem with these advanced tools is their restricted application, mainly intended for use during the design stage of the unit. In this sense, using empirical models can provide greater flexibility by increasing the number of possible scenarios where they can be applied.

Related to the equation-fit model, they are commonly developed as black-box models by regression analysis and experimental data. The main advantages of these typologies are a higher prediction accuracy for the adjusted experimental domain and a very low computational time. Fortunately, the unit performance is continuous with only smooth trends, so polynomial models are usually efficient functionals to describe them. In this sense, compressors, which are the basis for the heat pump performance, are very well studied in such types of empirical models. It is well known that AHRI polynomials [9] can characterize their performance ($\dot{W}_c$, $\dot{m}_{ref}$) by using a 10-term and third degree polynomial as a function of condensing and evaporating temperatures. Latest studies [10,11] have developed a more detailed analysis focused on the most appropriate polynomial model, obtaining more compact models with the same accuracy but depending on evaporation and condensation pressures. In the compressor field, evaporation and condensation temperatures or pressures can be suitable parameters if the main objective is to develop a compressor model that can be implemented as a model component. But, to develop a polynomial model for heat pump performance, the main problem is that these variables are internal parameters and therefore unknown (commonly, such measurements are only monitored in research). However, evaporation and condensation temperatures are dependent on boundary conditions at the evaporator and condenser side. Therefore, polynomials based on the external parameters, i.e., source/sink temperatures, should be able to characterize the unit performance.

Allen [12] already presented the idea of employing second-order polynomials with the evaporator and condenser outlet temperatures (secondary fluid, T_{eo} and T_{co}) to predict the full load performance (evaporator capacity and energy consumption of chillers, $\dot{Q}_e$ and $\dot{W}_c$). For example, the evaporator capacity was defined by adjusting Eqs. (1) and (2).

$$\dot{Q}_e = a_0 + a_1 T_{eo} + a_2 T_{co} + a_3 T_{eo} T_{co} + a_4 T_{eo}^2 + a_5 T_{co}^2 \quad (1)$$

And in a similar way, the energy consumption:

$$\dot{W}_c = b_0 + b_1 T_{eo} + b_2 T_{co} + b_3 T_{eo} T_{co} + b_4 T_{eo}^2 + b_5 T_{co}^2 \quad (2)$$

where the coefficients a_i and b_i are calculated by regression adjustment to experimental results.

Thus, this simple kind of model can provide the ability to include the heat pump unit as a simple component when a more complex system layout must be implemented. As reported by [13], such *"map-based"* models are most widespread in dynamic simulation programs like TRNSYS, ESP-r, EnergyPlus, and MATLAB/Simulink.

Similarly to Allen's model, other authors have published other polynomial models. For example, Tabatabaei [14] characterize the performance in air source heat pumps as a function of air temperature. Afjei [15] provided similar functions to Hamilton implemented as TRNSYS type, but for heat pump applications (prediction of condenser capacity and energy consumption). This same methodology is employed inside EnergyPlus [16], for the evaporator capacity, while for the consumption, a polynomial for the Energy Input to cooling output Ratio (EIR), i.e., the inverse of COP, was employed instead of energy consumption (Eqs. (3) and (4)). The output of these correlations is multiplied by the reference performance to give the full-load cooling capacity or energy consumption at specific temperature operating conditions (i.e., at temperatures different from the reference temperatures):

$$\frac{\dot{Q}_e}{\dot{Q}_{e,reference}} = a_0 + a_1 T_{eo} + a_2 T_{ci} + a_3 T_{eo} T_{ci} + a_4 T_{eo}^2 + a_5 T_{ci}^2 \quad (3)$$

$$\frac{EIR}{EIR_{reference}} = b_0 + b_1 T_{eo} + b_2 T_{ci} + b_3 T_{eo} T_{ci} + b_4 T_{eo}^2 + b_5 T_{ci}^2 \quad (4)$$

However, the main problem with these kind of models is that they only take into account the variation of the inlet (or outlet) temperatures of the secondary fluid to the evaporator and the condenser. So, the space of the independent variables domain is only 2D. As is described above, the usual procedure used by these authors was to characterize the performance at full load and then apply a correction for part load operation.

Unfortunately, new refrigeration and heat pump units are currently incorporating variable speed compressors and also variable speed circulation pumps and fans. Therefore, the characterization of new and future equipment with so many independent variables must be include more than two independent variables. In this sense, only a few authors have included improvements to the previous models. Ruschenburg [17], according to results in [18], updated Afjei's model considering the mass flow change in sink. So, Ruschenburg also defined second-order polynomials selecting the evaporator inlet temperature and substituting the condenser outlet by the condenser mean temperature to predict the condenser capacity and COP in heat pump applications (Eqs. (5) and (6)).

$$\dot{Q}_c = a_0 + a_1 T_{eo} + a_2 T_{c,mean} + a_3 T_{eo} T_{c,mean} + a_4 T_{eo}^2 + a_5 T_{c,mean}^2 \quad (5)$$

$$COP = b_0 + b_1 T_{eo} + b_2 T_{c,mean} + b_3 T_{eo} T_{c,mean} + b_4 T_{eo}^2 + b_5 T_{c,mean}^2 \quad (6)$$

On the other hand, the studies from [19,20] provide correlations including compressor speed as an additional variable. In [20], the functionals obtained for air source heat pumps were second-order polynomials as a function of condenser outlet temperature, air inlet temperature and compressor speed (Eqs. (7) and (8)).

$$\dot{Q}_c = a_0 + a_1 T_{ai} + a_2 T_{co} + a_3 f_c + a_4 T_{ai} T_{co} + a_5 f_c T_{ai} + a_6 f_c T_{co} + a_7 T_{ai}^2 + a_8 T_{co}^2 + a_9 f_c^2 \quad (7)$$

$$\dot{W}_c = b_0 + b_1 T_{ai} + b_2 T_{co} + b_3 f_c + b_4 T_{ai} T_{co} + b_5 f_c T_{ai} + b_6 f_c T_{co} + b_7 T_{ai}^2 + b_8 T_{co}^2 + b_9 f_c^2 \quad (8)$$

As we can see, the current models in the literature include from 1 to 3 independent variables. Unfortunately, this number of parameters is still insufficient because current units with variable speed components have a 5D domain (compressor speed, sink/source temperatures, and sink/source mass flow rate).

On the other hand, it is important to remark on the importance of using simple and compact models in heat pump applications. For example, the use of dynamic models allows the analysis of different control strategies [21–25] to optimize performance for air conditioning systems in buildings depending on the cooling and heating demands and the climatic region. Such dynamic models require direct feedback related to the heat pump component, where the abovementioned polynomial models can be implemented in a simple way predicting the heat pump performance depending on the external parameters. Another interesting challenge can also be using these models as soft-sensors [26] or for fault detection [27–30]. In the first case, the use of pre-fitted polynomial equations allows substituting physical sensors, such as electrical power meters or Coriolis flow meters, by predicting the electrical energy consumption or condenser and evaporator capacities with the polynomial models and complementing the information monitored in real installations. On the other hand, if these physical sensors are available, these measurements can be compared with the value provided by the pre-fitted polynomials and obtain direct feedback between the expected performance for a specific value of the external variables and the current performance measured, allowing to detect possible deviations caused by faults.

Against this background, the present study aims to analyze the most suitable polynomial models to predict the performance in current units considering this increase in the number of independent variables. They will be developed as a function of the external parameters in order to increase applicability. In this sense, this work aims to answer relevant questions such as which are the external variables to be included in the polynomial model depending on the operating mode, analyze the performance dependence on the selected external variables, and determine the most appropriate polynomial expressions to minimize prediction errors. The unit selected in this analysis is a new prototype of Dual Source Heat Pump (DSHP) with reverse cycle capability. Some questions regarding how this new typology of unit works will be included in the study to improve the understanding of how the models have been developed. As will be seen in the following sections, the operating modes in which the unit operates can be extrapolated to the main types of heat pumps and chillers currently available on the market (air source and ground source equipment). Consequently, this study is not only focused on modeling a specific unit, allowing the results of this work to be extended to other types of units and providing relevant results to the heat pump field.

2. Methodology

As already shown in Section 1, the topic analyzed in this work is at present poorly developed. It comprises a limited number of publications by some authors considering very simple units with a limited number of boundary variables. As previously mentioned, current units include a large number of variable speed components and the number of independent variables that determine the unit performance has increased. Therefore, the main problem is that there is currently no clear methodology for characterizing units with a large number of independent variables. In the field of current heat pump units, these variables include, for example, the frequency of the compressor, selected by the unit to cover the required user demand, or the supply temperature to the building, whose value will depend on the thermal load to be compensated and the season of the year.

Another challenge is the required information. The development of accurate polynomial models requires a huge dataset to describe the behavior of the unit under different working conditions. They allow the unit performance to be characterized over the entire working map.

As will be described below, the first problem when characterizing systems with 5 variables is the size of the experimental sample to be obtained. The second problem is that we need to know the type of mathematical expression to use in the polynomial model, which will be defined mainly by the relationship between the independent variables and the variables we wish to characterize (response variables). Therefore, to be sure of using an adequate polynomial model, an ideal scenario would be to generate the complete performance maps for the unit characterized.

Unfortunately, this implies considering a high number of levels in the independent variables and performing a fine mesh grid of points for the experimental domain considering a complete full factorial test plan. For example, selecting a system with 5 independent variables and 5 levels would produce a total of 3125 experimental test points. This means that the required experimental matrices include a large number of points and, in most cases, are impossible to obtain in the laboratory due to limited economic resources and time.

Due to the abovementioned problems, the approach used in this work has been to substitute the classical experimental campaigns with simulation results. For this purpose, the commercial software IMST-ART was selected to obtain a detailed model of the DSHP by modeling its internal components. By using this detailed model, the complete performance maps of the unit were generated for the analysis of the performance dependence with the external variables in order to explore the best polynomial expressions and adjust them to the simulated results. The prediction errors for the final models have been evaluated by using the Maximum Relative Error (MRE), the Root Mean Square Error (RMSE) and the Coefficient of Variation of the RMSE (CV_{RMSE}), i.e. the ratio of the RMSE to the mean of the response variable. Since this paper aims at generating the models from simulated results, there is no final adjustment to experimental data. This will be part of a future research work, where the polynomial models presented here will be complemented with an analysis of how to set up the experimental matrices and where to place the test points in the working domain by using Design of Experiments methodologies (DoE), and how to readjust the models of this work using experimental results to increase its accuracy.

A brief summary of the following sections is presented in order to assist the reader in understanding how this work is structured. Section 3 includes a brief description of the DSHP, highlighting the possible operating modes and the working range of the unit. Section 4 briefly describes how the detailed model of the DSHP was developed in the IMST-ART software necessary to generate the simulation results. Finally, Section 5 includes a complete description of how the polynomial models have been obtained and Section 6 a brief summary of the prediction errors.

3. DSHP unit

GSHP (Ground Source Heat Pump) systems have demonstrated superior efficiency compared to traditional air-to-water heat pumps. Urchueguía [31] conducted research and found that GSHP systems can lead to an impressive reduction of up to 40% in annual electricity consumption compared to conventional air-to-water heat pumps. Nevertheless, a primary challenge with GSHPs is their substantial initial investment cost. In this sense, an alternative strategy involves integrating GSHP systems with an additional thermal source through hybrid systems. The Dual Source Heat Pump analyzed in this work, which combines ground and air as heat sources, offers two fundamental benefits. Firstly, by incorporating an air heat exchanger, it becomes possible to significantly reduce the size of the ground heat exchanger, leading to a notable reduction in the overall system cost. Secondly, by optimizing the system's operation, the flexibility to choose the most appropriate heat source can result in a significantly improved seasonal performance, removing for instance defrost cycles typically required in air source heat pumps installed in cold regions.

Table 1
DSHP components.

Component	Manufacturer	Hydraulic loop	Size
Compressor XHV-025[a]	Copeland	–	25 cm^3
BPHE F85	SWEP	User	1.08 m^2
BPHE F80AS	SWEP	Ground	1.08 m^2
BPHE B26	SWEP	DHW	0.656 m^2
RTPFHx	–	Air	38.56 m^2
Liquid receiver	–	–	6.6 l
EEV E2V14	Carel	–	8.3 kW (R410a)

[a] Originally designed for R410A. Oil changed to POE32 according to manufacturer's recommendations.

The DSHP analyzed in this work is one of the three prototypes designed inside the framework of the GEOTeCH project [32]. Specifically, this first prototype helped set an initial design to improve subsequent prototypes. Some of the main problems were defining a suitable interconnection typology and their manage for the internal components – finally implemented on the refrigerant side – the number of heat exchangers required according to the desired operating modes, and sizing the components for the required nominal heating capacity defined in the project. The main characteristics of this first prototype are the following:

- Reversible unit with Plug&Play construction.
- Domestic Hot Water (DHW) production.
- Nominal heating capacity: 8 kW.
- Refrigerant: R32.

In particular, this prototype was designed by the Italian company HiRef [33] in collaboration with the Institute for Energy Engineering (IUIIE) located at the Polytechnic University of Valencia (UPV). This unit includes a Round Tube Plate Fin Heat exchanger (RTPFHx) and three Braze Plate Heat Exchangers (BPHEs) connected in parallel with a suitable interconnection of solenoid valves and check valves in the refrigeration circuit. This configuration allows selection of the desired source/sink interconnecting the Heat eXchangers (HXs) with an inverter scroll compressor and the Electronic Expansion Valve (EEV). Additionally, a liquid receiver is installed at the condenser outlet to store any liquid refrigerant that will be excess to requirements in some modes and operating conditions. Therefore, the HP operates with a subcooling of ≈0 K and the EEV sets a constant superheat of 5 K at the suction pipe. The current design makes the unit especially flexible, being able to switch the most advantageous source from an efficiency point of view – especially in medium climates – and including variable speed components to adapt to different heating loads and different temperature variations efficiently. Table 1 shows a summary of the main components installed in this unit and Fig. 1 includes the final Plug&Play solution. The following two subsections will show the temperature ranges in which this machine can work and the operating modes available in this unit and depending on the operating conditions and the selected source/sink.

3.1. Operating conditions

The operating conditions of the DSHP have been set in terms of user side and source/sink side, as they were defined in the Deliverable 4.1 [34] of the GEOTeCH [32] project, Table 2.

These temperature values are used to define the range conditions that need be evaluated to characterize the performance of this unit and they represent the maximum temperature range in which the system will work.

As an example, for low temperature heating (radiant floor), the water temperature to the user side (production of the heat pump) is expected to be somewhere between 35 and 40 °C. In this situation, when the ground source is selected, the brine temperature to the heat

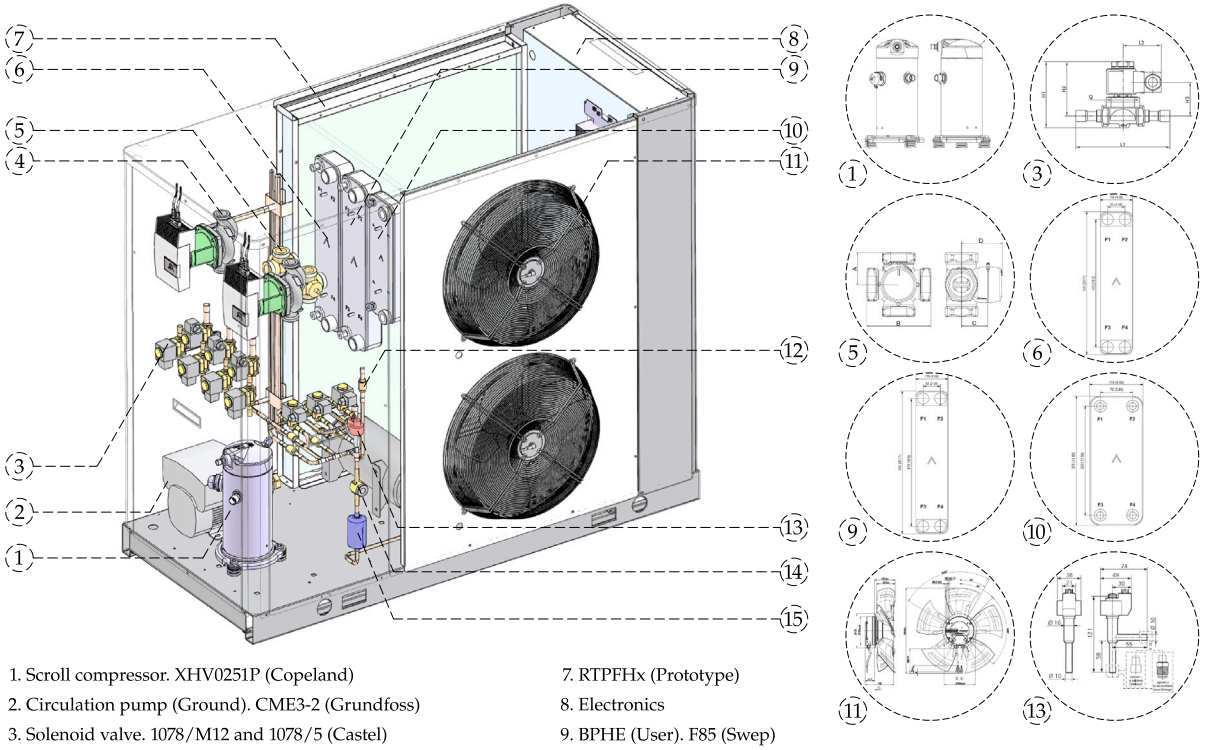

1. Scroll compressor. XHV0251P (Copeland)
2. Circulation pump (Ground). CME3-2 (Grundfoss)
3. Solenoid valve. 1078/M12 and 1078/5 (Castel)
4. Circulation pump (User/DHW). Stratos Para 25/1 (Wilo)
5. 4-way valve. VRG142+ARA632 (ESVE)
6. BPHE (Ground). F80AS (Swep)
7. RTPFHx (Prototype)
8. Electronics
9. BPHE (User). F85 (Swep)
10. BPHE (DHW). B26 (Swep)
11. Fans. A3G450-AC28-51 (EBM)
12. Check valves. 3132/M10 (Carel)
13. EEV. E2V24 (Carel)
14. Sight glass
15. Filter drier

Fig. 1. DSHP unit.

Table 2
Operating conditions (secondary fluid values)[a].

Primary operation (Secondary operation is DHW with user side 50–55 °C)	User Temp. (°C)	Source/sink Temp. (°C) (COLD CLIMATE)		Source/sink Temp. (°C) (WARM CLIMATE)	
		Ground	Air	Ground	Air
Heating-low temperature (radiant floor)	35/40	−5/10	5/15	5/20	5/20
Heating-medium temperature (convector/radiator)	40/45	−5/10	5/15	5/20	5/20
Heating-high temperature (radiator)	45/55	−5/10	5/15	5/20	5/20
Winter-DHW	50/55	−5/10	5/20	5/20	5/25
Cooling-high temperature (radiant surface)	18/26	10[b]/30	18/30	10/35	18/40
Cooling-medium temperature (air handling)	12/16	10[b]/30	18/30	10/35	18/40
Cooling-low temperature (air handling & dehumidification)	6/10	10[b]/30	18/30	10/35	18/40
Summer-DHW	50/55	10[b]/30	18/30	10/35	18/40

[a] User temp. defined as supply temp. and ground and air temp. as return (borehole) and air inlet (coil) temp.
[b] Free-cooling for brine temperatures below 10 °C.

pump is expected to vary between −5 and 10 °C (cold climate), and between 5 and 15 °C in the air, when the heat pump works with the air source.

3.2. Operating modes

In order to cover all demands, the DSHP is able to operate in nine different working modes, which are summarized in Table 3. They are primarily classified depending on the season: when the system operates in summer mode, it will work as a chiller; when it operates in winter mode, it will work as a heat pump.

The unit is also able to operate in free-cooling conditions when the return temperature from the borehole loop is lower than 10 °C. However, this extra mode is not included in Table 3 because in this condition, the unit is switched off and the present work only analyzes the working maps of the unit. Moreover, modes 6S, 6W and 7S and 7W corresponds to the same type of heat pump, i.e, the unit works with the same heat exchangers as condenser and evaporator, but in different season. Modes 6S and 6W corresponds to domestic hot water production selecting the air as source. Modes 7S and 7W supplies also domestic hot water but selecting the ground as source. Therefore there are a total of 7 different operating modes if we consider only the different heat exchanger connection when the unit selects the condenser and evaporator.

According to Table 3, the unit is provided with three Brazed Plate Heat Exchanger (BPHEs) to cover the User and DHW demands and for the heat transfer in the Ground side. Then, a Round Tube Plate Fin Heat exchanger (RTPFHx) is also installed for the heat transfer in the air side.

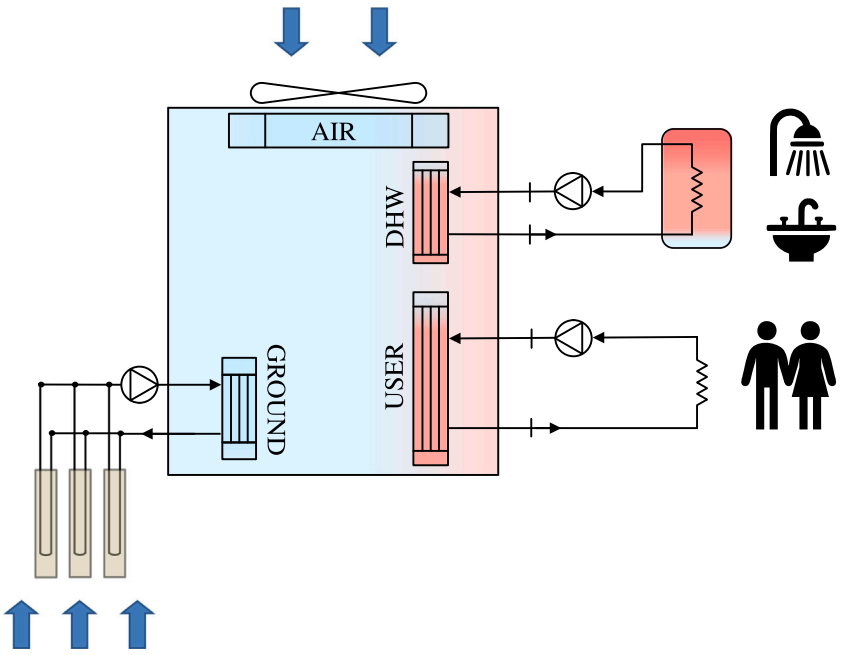

Fig. 2. DSHP basic diagram.

Table 3
Operating modes.

Mode	Summer		Mode	Winter	
	Condenser	Evaporator		Condenser	Evaporator
Heating & Cooling					
1-SA[a]	Air	User	4-WA[f]	User	Air
2-SG[b]	Ground	User	5-WG[g]	User	Ground
DHW & Cooling					
3-DHWU[c]	DHW	User			
Domestic Hot Water					
6S-DHWA[d]	DHW	Air	6W-DHWA[d]	DHW	Air
7S-DHWG[e]	DHW	Ground	7W-DHWG[e]	DHW	Ground

[a] SA: Summer Air.
[b] SG: Summer Ground.
[c] DHWU: Domestic Hot Water User.
[d] DHWA: Domestic Hot Water Air.
[e] DHWG: Domestic Hot Water Ground.
[f] WA: Winter Air.
[g] WG: Winter Ground.

Fig. 2 shows a simple diagram of the DSHP including the appointed heat exchangers.

Finally, a brief description is given below for the 9 operating modes to better understand how the unit works:

- Mode 1: SUMMER (AIR). The unit is working as a chiller, so producing chilled water at the internal heat exchanger (USER in Fig. 2). Condensation occurs at the air-to-refrigerant Heat eXchanger (HX) (AIR in Fig. 2).
- Mode 2: SUMMER (GROUND). The unit is working as a chiller, so producing chilled water at the internal heat exchanger (USER in Fig. 2). Condensation occurs at the brine-to-refrigerant HX (GROUND in Fig. 2).
- Mode 3: SUMMER (DHW - USER). The unit is working as a chiller, so producing chilled water at the internal heat exchanger (USER in Fig. 2). Condensation occurs at the dedicated BPHE (DHW in Fig. 2). The nomenclature DHW - USER refers to the fact that the DHW is produced employing the USER (internal circuit) as the heat source. In this mode, the system is producing chilled water and DHW at the same time. The DHW production is therefore conditional on the existence of the cooling load.
- Mode 4: WINTER (AIR). The unit is working as a heat pump, so producing hot water at the internal heat exchanger (USER in Fig. 2). Evaporation occurs at the air-to-refrigerant HX (AIR in Fig. 2).
- Mode 5: WINTER (GROUND). The unit is working as a heat pump, so producing hot water at the internal heat exchanger (USER in Fig. 2). Evaporation occurs at the brine-to-refrigerant HX (GROUND in Fig. 2).
- Mode 6S: SUMMER (DHW - AIR). The unit is working in summer conditions as a heat pump, so producing DHW at the dedicated BPHE (DHW in Fig. 2). Evaporation occurs at the air-to-refrigerant HX (AIR in Fig. 2). The nomenclature DHW - AIR refers to the fact that the DHW is produced employing AIR as the heat source. DHW production is therefore independent of the building's thermal load with no chilled water production.
- Mode 7S: SUMMER (DHW - GROUND). The unit is working in summer conditions as a heat pump, so producing DHW at the dedicated BPHE (DHW in Fig. 2). Evaporation occurs at the brine-to-refrigerant HX (GROUND in Fig. 2). The nomenclature DHW - GROUND refers to the fact that the DHW is produced employing the brine coming from the ground as the heat source. DHW production is therefore independent of the building's thermal load with no chilled water production.
- Mode 6W: WINTER (DHW - AIR). The unit is working in winter conditions as a heat pump, so producing DHW at the dedicated BPHE (DHW in Fig. 2). Evaporation occurs at the air-to-refrigerant HX (AIR in Fig. 2). This mode is identical to Mode 6S but the operating temperatures will be remarkably different.
- Mode 7W: WINTER (DHW - GROUND). The unit is working in winter conditions as a heat pump, so producing DHW at the dedicated BPHE (DHW in Fig. 2). Evaporation occurs at the brine-to-refrigerant HX (GROUND in Fig. 2). This mode is identical to Mode 7S but the operating temperatures will be remarkably different.

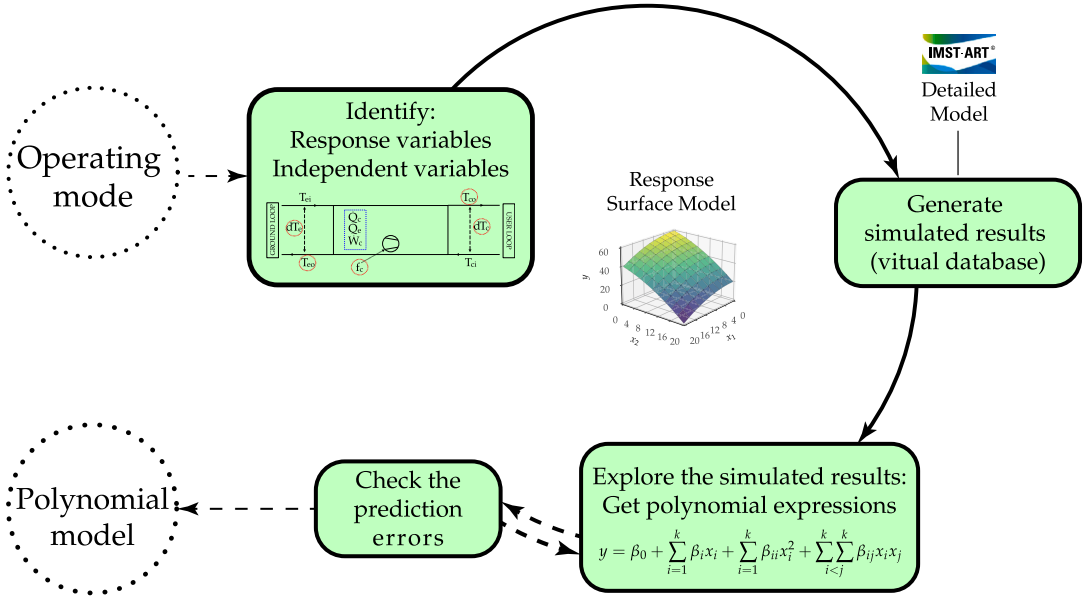

Fig. 3. Steps to obtain polynomial models.

4. DSHP detailed model

This section introduces the detailed model of the DSHP developed for each operating mode in the commercial simulation tool IMST-ART. The main objective of this detailed model was to generate the complete working maps of the unit as a virtual test and then, to find better empirical equations for the characterization of the unit performance. The simulation software used is IMST-ART but any other simulation software can be generally considered to obtain simulation data for the complete unit map (e.g., VapCyc or CYCLE_D-HX). This tool has been validated in many studies, such as [35–38], where the experimental results for different HP technologies have been compared with experimental tests conducted in the laboratory under steady-state conditions. Commonly, the prediction errors in IMST-ART are between 5% and 10% of MRE when comparing performance simulation results with experimental results. As concerns the DSHP detailed model, it was implemented by being provided with all the geometric and performance data for the individual components installed in the DSHP to IMST-ART (compressor, HX, etc.). As mentioned above, the DSHP can operate 7 working modes. Therefore, seven models were implemented in the IMST-ART software selecting the corresponding heat exchangers available in each operating mode.

The data for every individual component was extracted from the manufacturers' catalogs. Manufacturers usually have their own software where they include information related to their products, for example, the performance curves of circulation pumps [39,40], the geometric parameters and performance of heat exchangers [41], or the swept volume, energy consumption, and mass flow rate of the compressor [42]. The option selected for the compressor submodel was to introduce the compressor performance as AHRI polynomials, including the compressor frequency as an additional independent variable. The model reported by [43] – suitable for rotary compressors and also for scroll compressors [10] – was selected for this purpose. It includes the following functionals:

First of all, a nominal frequency (50 Hz) is selected adjusting Eqs. (9) and (10) for the prediction of the compressor power input ($\dot{W}_c^*$) and the mass flow rate ($\dot{m}_{ref}^*$) at this frequency as a function of the condensing and evaporating temperatures (T_c and T_e):

$$\dot{m}_{ref}^* = a_0 + a_1 T_e + a_2 T_c + a_3 T_e T_c + a_4 T_e^2 + a_5 T_c^2 \tag{9}$$

$$\dot{W}_c^* = b_0 + b_1 T_e + b_2 T_c + b_3 T_e T_c + b_4 T_e^2 + b_5 T_c^2 \tag{10}$$

The equations above includes the main terms of the map-based models defined in the standard [9]. These terms are the linear predictors (T_e, T_c), quadratic terms (T_e^2, T_c^2) and the first order interaction term ($T_e \times T_c$) of the condensation temperature and the evaporation temperature.

Then, Eqs. (11) and (12) correct the other compressor frequencies (f_c) to the performance at the nominal frequency (f_c^*):

$$k_M = \frac{\dot{m}_{ref}}{\dot{m}_{ref}^*} = c_0 + c_1(f_c - f_c^*) + c_2(f_c - f_c^*)^2 \tag{11}$$

$$k_P = \frac{\dot{W}_c}{\dot{W}_c^*} = d_0 + d_1(f_c - f_c^*) + d_2(f_c - f_c^*)^2 \tag{12}$$

Finally, in order to introduce the compressor submodel in ART, the abovementioned equations were recomposed as a set of second-order AHRI polynomials by considering different discretized levels for the value of the compressor speed.

5. DSHP polynomial models

Once the operation of the DSHP and the detailed model developed to generate the operating maps have been introduced, this section will focus on performing the polynomial models from the analysis of the simulation results. It includes the best strategy for selecting the independent variables, the range covered in the simulation maps, and an analysis of the observed trends ending with the model construction. A simple representation of the abovementioned workflow is represented in Fig. 3.

5.1. Response variables and independent variables in the DSHP

The performance of a vapor compression heat pump or refrigeration equipment is characterized by three response variables: condenser capacity ($\dot{Q}_c$), evaporator capacity ($\dot{Q}_e$) and compressor or unit energy consumption ($\dot{W}_c$ or $\dot{W}_{HP}$).

At the same time, in variable speed units, the value of the performance will be a function of the compressor frequency (f_c) and the operating conditions at the evaporator and condenser heat exchangers (HXs). Therefore, the independent variables to model the performance are the compressor frequency and a set of variables that fix the boundary conditions for the condenser and the evaporator.

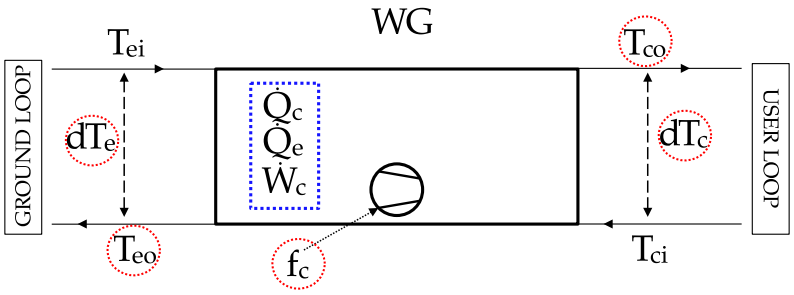

Fig. 4. Winter Ground: Response and control variables.

Regarding the boundary conditions in the HX, there are two possible approaches in order to select the independent variables this includes:

On the one hand, we can select the independent variables in the primary loop as evaporation and condensation temperatures. This is the common approach used, for example, in the characterization of the main component in HPs, the compressor. Nevertheless, the use of condensation and evaporation temperatures has the disadvantage of needing measurements in the refrigerant loop. These measurements are monitored by researchers in the laboratory but they are not usually available in real installations.

Then, on the other hand, another approach is to select the independent variables in the secondary loop. In this situation, the boundary conditions for the condenser or evaporator are characterized by only two independent variables, and these variables can be any combination of the three variables controlled in the secondary loops: inlet and outlet temperatures, and mass flow rate. This corresponds to the normal operation of these units. The source/sink conditions and user demand, together with the compressor frequency, set the condensation and evaporation temperatures in the refrigerant loop.

Therefore, due to the fact that secondary loop variables are usually monitored in real installations and are easy to measure, they will be selected as independent variables in order to construct the final correlations for the characterization of the performance in this unit. In this sense, the final models will depend only on the external variables, which will make it easier to use in many possible scenarios.

Now, we are going to identify the set of independent variables for the DSHP. The following subsection describes the independent variables involved in the process for the main operating modes, Winter Ground or Winter Air modes, when the DSHP works as a brine-to-water HP or air-to-water HP.

5.1.1. *Winter ground and winter air modes*

Fig. 4 shows a schematic diagram for Winter Ground mode including the independent variables in the hydraulic loops (User and Ground loops), the response variables of interest ($\dot{Q}_c$, $\dot{Q}_e$ and $\dot{W}_c$) and the compressor frequency (f_c).

In this operating mode, the HP works as a geothermal HP. For that reason, the independent variables are the compressor frequency, the mass flow rate in the hydraulic loops (controlled by the frequency of the circulation pumps), the return temperature in the Ground BPHE (T_{ei}, this is the brine return temperature from the borehole HX) and the supply temperature in the User BPHE (T_{co}, this is the hot water supply temperature to the building).

This set of 5 independent variables can be selected in order to model the performance of the unit. However, the independent variables highlighted in red in the figure above were the independent variables selected to model the performance in this operating mode.

The temperature difference across the BPHE (dT_c and dT_e) in the secondary loops was selected rather than the mass flow rate because, in real installations, the inlet and outlet temperatures are usually always measured and monitored while mass flow rate is seldom measured. This is an equivalent representation of the mass flow rate in the secondary loops. When we increase or decrease the velocity of the circulation pumps, the values of dT_c and dT_e also decrease or increase for a given capacity. Both dT_c and dT_e are defined as positive, i.e. $dT_c = T_{co} - T_{ci}$ and $dT_e = T_{ei} - T_{eo}$.

Additionally, the outlet temperature in the secondary side of the BPHE (T_{eo}) was also selected rather than T_{ei} in the evaporator and keeping T_{co} in the condenser. Due to the fact that the BPHEs in this unit always work in counter-current, the secondary outlet temperatures are a better representation of the evaporation or condensation temperatures, which set the refrigerant conditions in the HXs and therefore the performance of the unit.

Selecting the 5 independent variables described above (f_c, T_{eo}, dT_e, T_{co} and dT_c), Eqs. (13)–(15) allow to the performance of the DSHP to be calculated to include the effect of the auxiliary components:

Winter Ground - Performance including the auxiliary components

$$\dot{Q}_{heating} = \dot{Q}_c(f_c, T_{eo}, dT_e, T_{co}, dT_c) + \left[\eta_p \cdot \dot{W}_{user,pump} - P_{h,user}\right] \quad (13)$$

$$\dot{Q}_{cooling} = \dot{Q}_e(f_c, T_{eo}, dT_e, T_{co}, dT_c) - \left[\eta_p \cdot \dot{W}_{ground,pump} - P_{h,ground}\right] \quad (14)$$

$$\dot{W}_{DSHP} = \dot{W}_c(f_c, T_{eo}, dT_e, T_{co}, dT_c) + \dot{W}_{par} + \dot{W}_{user,pump} + \dot{W}_{ground,pump} \quad (15)$$

On the one hand, the variables $\dot{Q}_{heating}$ and $\dot{Q}_{cooling}$ are the capacities including the heat injected by the circulation pumps, where $\dot{Q}_{heating}$ rejects the heat from the condenser to the User and $\dot{Q}_{cooling}$ absorbs the heat from the Ground in the evaporator. Then, $\dot{W}_{DSHP}$ is the total electrical consumption of the unit and it is calculated by adding the parasitic and circulation pumps consumption to the compressor energy consumption.

On the other hand, the highlighted parts in the equations above are the variables $\dot{W}_c$, $\dot{Q}_c$ and $\dot{Q}_e$ and they exclude the effect of the auxiliary components. As mentioned above, they have been selected as response variables to obtain the empirical models reported in this work. If we exclude the effects of the auxiliary components over the response variables, we will simplify the construction of the response models. Related to these effects, only implies a minor correction over $\dot{W}_c$, $\dot{Q}_c$, and $\dot{Q}_e$ parameters. The characterization of the auxiliary components is also included in the supplementary material, and the equations above together with the expressions defined in the supplementary material allows the effect of the auxiliary components to be included in the empirical models developed.

Now, setting aside the Winter Ground mode and focusing on the Winter Air mode, Fig. 5 shows the variables involved in the process when the unit works as an air-to-water HP.

This figure includes the same independent variables selected in Winter Ground with the exception of the variables which relate to the evaporator. In Winter Air, the unit works with the Round Tube Plate Fin Heat Exchanger (RTPFHx) as the evaporator and therefore the variables

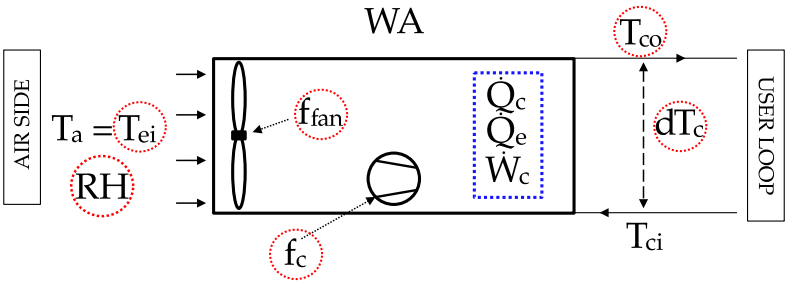

Fig. 5. Winter Air: Response and control variables.

T_{eo} and dT_e are replaced by the air temperature at the inlet of the RTPFHx (T_{ei}) and the frequency of the fan (f_{fan}). Furthermore, the relative humidity (RH) is an extra variable to take into account.

Due to the fact that the RTPFHx works as an evaporator, it may involve condensation of humid air – sensible and latent capacity – on the heat transfer surfaces when the external wall surfaces of the round tubes are below the corresponding dew point temperatures. As will be seen in Section 5.4, the inclusion of RH as an extra independent variable will be necessary in the calculation of the capacities and it is excluded from the compressor energy consumption.

Taking into account the selected independent variables (f_c, T_{ei}, f_{fan}, RH, T_{co} and dT_c), Eqs. (16)–(18) are the expressions to calculate the performance including the effect of the auxiliary components:

Winter Air - Performance including the auxiliary components

$$\dot{Q}_{heating} = \boxed{\dot{Q}_c(f_c, T_{ei}, f_{fan}, RH, T_{co}, dT_c)} + \left[\eta_p \cdot \dot{W}_{user,pump} - P_{h,user}\right] \tag{16}$$

$$\dot{Q}_{cooling} = \boxed{\dot{Q}_e(f_c, T_{ei}, f_{fan}, RH, T_{co}, dT_c)} \tag{17}$$

$$\dot{W}_{DSHP} = \boxed{\dot{W}_c(f_c, T_{ei}, f_{fan}, T_{co}, dT_c)} + \dot{W}_{par} + \dot{W}_{user,pump} + \dot{W}_{fan} \tag{18}$$

In this case, the electrical consumption of the circulation pump in the evaporator side is replaced by the electrical consumption of the fan. Eq. (17) can also be corrected by the heat injected of the fan. However, in order to simplify the expression and following the guidelines of the BS EN Standard 14511-3:2018 [44], a correction of the capacity with the heat injected by fans is not required (It is expected to be low).

Then, like Winter Ground mode, the highlighted parts in the equations above ($\dot{W}_c$, $\dot{Q}_c$ and $\dot{Q}_e$) will be the response variables correlated in Winter Air mode and they exclude the effect of the auxiliary components. The supplementary material also includes the characterization of the fan.

5.1.2. Summer and DHW modes

The subsection above analyzes the independent variables selected in the main operating modes, Winter Ground and Winter Air. As concerns the remaining operating modes, Summer Ground, DHW Ground and DHW User modes operate with two BPHEs as evaporator and condenser (brine-to-water or water-to-water HP).

They will have the same schematic diagram as Winter Ground (Fig. 4) but work with the corresponding hydraulic loops selected in each operating mode (see Section 3.2). Therefore, they will include the same independent variables as Winter Ground mode. Eqs. (13)–(15) must be modified to include the correction with the corresponding circulation pumps (this depends on the hydraulic loops selected).

Then, on the other hand, DHW Air mode operates with the RTPFHx as the evaporator including the same independent variables as Winter Air mode and replacing the User loop with the DHW loop in the condenser. Eqs. (16) and (18) must be modified including the correction with the circulation pump in the DHW loop.

Finally, Fig. 6 is the schematic diagram for Summer Air mode, and the only difference from Winter Air mode is that now the condenser is the RTPFHx and the evaporator is the User BPHE. Therefore, it will include the independent variables f_c, T_{eo}, dT_e, T_{ci} and f_{fan}. The relative humidity is not included as an independent variable because there are no dehumidification conditions when the RTPFHx works as a condenser.

Eqs. (19)–(21) are the expressions to calculate the performance including the effect of the auxiliary components in Summer Air mode:

Summer Air - Performance including the auxiliary components

$$\dot{Q}_{heating} = \boxed{\dot{Q}_c(f_c, T_{eo}, dT_e, T_{ci}, f_{fan})} \tag{19}$$

$$\dot{Q}_{cooling} = \boxed{\dot{Q}_e(f_c, T_{eo}, dT_e, T_{ci}, f_{fan})} - \left[\eta_p \cdot \dot{W}_{user,pump} - P_{h,user}\right] \tag{20}$$

$$\dot{W}_{DSHP} = \boxed{\dot{W}_c(f_c, T_{eo}, dT_e, T_{ci}, f_{fan})} + \dot{W}_{par} + \dot{W}_{user,pump} + \dot{W}_{fan} \tag{21}$$

5.2. Development of the virtual test database by using the DSHP detailed model

Once we have identified all the independent variables for the 7 operating modes, the second step is to look for the functionals that are able to predict the response variables ($\dot{Q}_c$, $\dot{Q}_e$ and $\dot{W}_c$) with the highest accuracy in the experimental domain.

For this purpose, researchers usually carry out experimental campaigns in order to characterize the performance of units, such as the characterization of refrigerating compressors in the 2-dimensional space defined by the condensation and evaporation temperatures [9].

However, as we have identified in the subsections above the experimental domain for new heat pumps and refrigeration equipment is increased because many of them incorporate variable speed compressors and also variable speed circulation pumps and fans. In the DSHP, this experimental domain is a 6-dimensional space in Winter Air and DHW Air modes – RH is an extra parameter – and a 5-dimensional space for the rest of operating modes (Winter Ground, Summer Ground, DHW Ground, DHW User and Summer Air).

Unfortunately, the characterization of equipment with so many independent variables cannot be completed exhaustively by experimentation because of the huge amount of data required. The definition of the experimental points to test will be a function of the number of independent variables and the number of levels selected for each one.

For example, if we consider the Winter Ground mode with 5 independent variables, we will obtain the following full factorial test plans:

- 3 levels for each variable ⇒ $3^5 = 243$ test points.
- 4 levels for each variable ⇒ $4^5 = 1024$ test points.
- 5 levels for each variable ⇒ $5^5 = 3125$ test points.

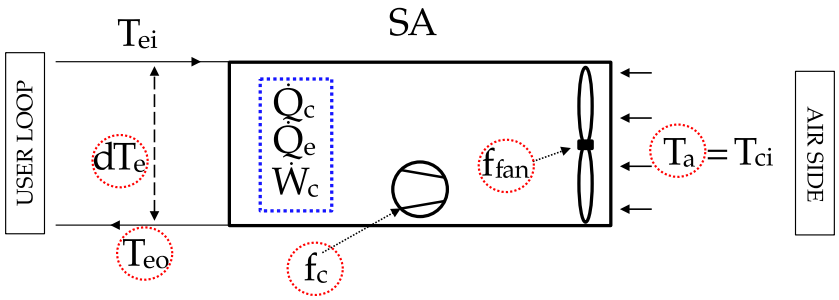

Fig. 6. Summer Air: Response and control variables.

Table 4
DSHP virtual tests.

f_c Hz	T_{co} or T_{ci} °C	dT_c or f_{fan} K or %	T_{eo} or T_{ei} °C	dT_e or f_{fan} K or %	Virtual tests[a]
SA: (f_c, T_{ci}, f_{fan}, T_{eo}, dT_e)					
[30, 40, 50, 60, 70]	[15, 21, 27, 33, 39]	[20, 35, 50, 65, 80]	[6, 9, 12, 15, 18]	[2, 3, 5, 7, 9]	3125
SG: (f_c, T_{ci}, dT_c, T_{eo}, dT_e)					
[30, 40, 50, 60, 70]	[6, 11, 16, 21, 26]	[2, 3, 5, 7, 9]	[6, 9, 12, 15, 18]	[2, 3, 5, 7, 9]	3125
DHWU: (f_c, T_{co}, dT_c, T_{eo}, dT_e)					
[30, 40, 50, 60, 70]	[50, 52, 55, 58, 60]	[5, 10, 20, 30, 40]	[6, 9, 12, 15, 18]	[2, 3, 5, 7, 9]	3125
WA: (f_c, T_{co}, dT_c, T_{ei}, f_{fan})					
[30, 40, 50, 60, 70]	[35, 40, 45, 50, 55]	[2, 3, 5, 7, 9]	[4, 7, 11, 15, 19]	[20, 35, 50, 65, 80]	3125
WG: (f_c, T_{co}, dT_c, T_{ei}, dT_e)					
[30, 40, 50, 60, 70]	[35, 40, 45, 50, 55]	[2, 3, 5, 7, 9]	[−5, 0, 5, 10, 15]	[2, 3, 5, 7, 9]	3125
DHWA: (f_c, T_{co}, dT_c, T_{ei}, f_{fan})					
[30, 40, 50, 60, 70]	[50, 52, 55, 58, 60]	[5, 10, 20, 30, 40]	[5, 11, 17, 23, 29]	[20, 35, 50, 65, 80]	3125
DHWG: (f_c, T_{co}, dT_c, T_{ei}, dT_e)					
[30, 40, 50, 60, 70]	[50, 52, 55, 58, 60]	[5, 10, 20, 30, 40]	[−5, 2, 10, 18, 25]	[2, 3, 5, 7, 9]	3125

[a] 5 levels for each of the 5 control variables ⇒ $5^5 = 3125$ virtual tests by operating mode ⇒ Total virtual tests: **21 875**.

Considering therefore that the performance dependence with each independent variable is not linear and it includes at least some curvature, the number of levels to be considered should be around 4 or 5. This results in really large experimental matrices with around 1000 or 3000 test points, and in this unit these amount of points must be tested in each of the 7 operating modes (around 7000 or 21000 test points). Of course, it would be completely unfeasible to conduct a full factorial plan, due to the significant amount of time and effort needed and an alternative approach is required. However, current simulation tools in the field of engineering bring us the opportunity to substitute experimentation with simulation results. This allow us to generate a huge amount of simulation data that would otherwise be impossible to obtain by experimentation.

In this sense, the detailed model of the DSHP implemented in the IMST-ART software was used to perform a virtual database with simulation data for the entire working maps of the DSHP. The generated database includes the full factorial for the 5 control variables, selecting 5 levels for each one.

Therefore, a high-resolution mesh grid of virtual tests for the response surfaces was generated, allowing us to explore the better polynomials to predict the HP performance.

Table 4 shows the levels selected – based on the operating ranges introduced in Section 3.1 – for the independent variables in order to simulate the full factorial plans and generate a virtual database with a total of **21 875 points**. The total number of virtual tests generated in IMST-ART can be obtained as the full factorial for the total number of control variables and their levels.

In Winter Air and DHW Air modes, the relative humidity was also included as an independent variable in the polynomial models to take into account the dehumidification process in the evaporator. However, in order to decrease the number of simulation points, it is not included in the full factorial, and the humidity conditions in the air are fixed as a dry and wet bulb temperature difference of 1 °C in air inlet temperatures of less than 11 °C. Then, the humidity ratio corresponding to the moist air conditions of 11(10) °C is fixed in air inlet temperatures greater than 11 °C.

According to the methodology described above, Section 5.3 explores the best functionals for the polynomial models by using the abovementioned virtual test database.

5.3. Exploring functionals with the virtual database

The development of an empirical polynomial model is not an easy task and it involves the use of statistical and graphical techniques in order to find a suitable functional to characterize the response variables of interest. As mentioned above, the response variables selected are $\dot{W}_c$, $\dot{Q}_c$ and $\dot{Q}_e$ and they will be characterized for the 7 operating modes. Therefore, we need to find 21 polynomial equations to characterize the performance of the DSHP. In order to describe the process appropriately and obtain the best polynomial equations, this section includes the construction of the polynomial models for the main operating mode, Winter Ground. Furthermore, Section 5.4 describes how to include the dehumidification effect in Winter Air for the characterization of the capacities. A summary for the final polynomial models developed in the 7 operating modes has been included as supplementary material.

5.3.1. Winter ground polynomial models

Starting with the characterization of the performance in Winter Ground mode, the first thing to do is to explore the relationship between the independent variables and the response variables.

Typically, matrix correlation plots are the most common graphs to show this. For example, selecting $\dot{W}_c$ to start the analysis, Fig. 7 provides the correlation matrix for this response variable.

It includes the following information:

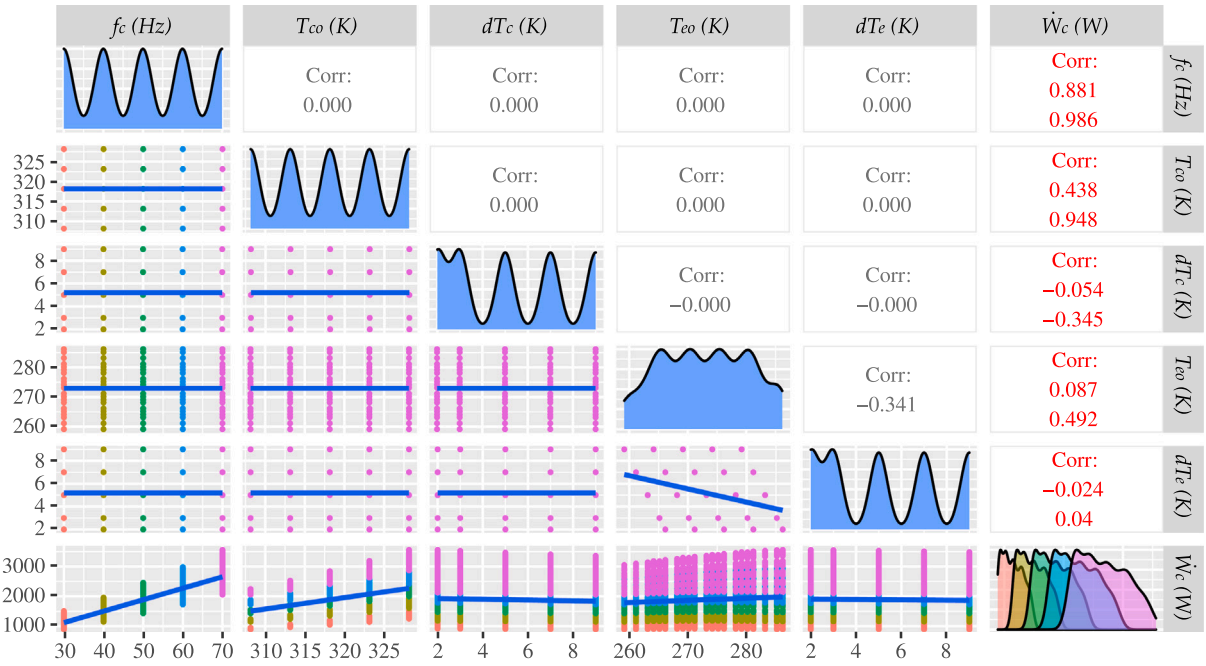

Fig. 7. WG: Correlation matrix $\dot{W}_c$.

- The density plots with the representation of the data distribution for the independent and response variables (the diagonal of the matrix). In these density plots, the y-axis is rescaled between 0 and 1, where the x-axis shows the data distribution for each variable. In this sense, the independent variables show a single density curve – we can observe the different levels considered – to simplify the visualization. On the other hand, several density curves have been included for each compressor frequencies in the response variable ($\dot{W}_c$, right lower corner plot). This will be useful later when analyzing transformations on the response variable to simplify the final models.
- Scatter plots with all the bivariate representations (at the lower part of the diagonal). It also includes a linear adjustment for all the data represented in each plot. These graphs are very useful for analyzing the various dependencies between the response and independent variables.
- Color series in the scatter plots. The selected variable to define the series is the compressor frequency (f_c). That is the main independent variable, as we will soon see.
- The correlation coefficient of Pearson (ccp) and the partial correlation coefficient of Pearson ($pccp$) (at the upper part of the diagonal). These coefficients measure the level of correlation between variables. They will be discussed in more detail later.
- Variable labels at the top (x-axis) and right side (y-axis). By combining them, we can identify: the variables considered on the scatter plot axes, the pair of variables to which the correlation coefficients refer, and the variable considered in the density plots.

As we can see, only the last row and column provides us with information about the relationship between $\dot{W}_c$ and the independent variables. The other plots are the combination between independent variables, and therefore it does not demonstrate any dependence. The only dependence is presented in the plot T_{eo} vs. dT_e. This is because the real boundary variable in the normal operation of the unit, and also the one selected to generate the full factorial in the virtual test, is T_{ei} ($T_{eo} = T_{ei} - dT_e$).

However, we obtained better results in the performance characterization when we took T_{eo} as the independent variable rather than T_{ei}. As previously discussed, the secondary outlet temperatures are a better representation of the evaporation and condensation temperature when the BPHE work in counter-current, so we took T_{eo} as the independent variable rather than T_{ei}, and therefore it is included in the correlation matrix.

First, we are going to analyze the results of the statistical coefficients of Pearson. These two coefficients measure the relationship between two continuous variables and show how strong this is. The value varies between −1 and 1, with the following results:

- 1 indicates a strong positive relationship.
- −1 indicates a strong negative relationship.
- A result of zero indicates no relationship at all.

This helps us to identify which are the most important independent variables. As given in Fig. 7, the main independent variable that fixes the value of $\dot{W}_c$ is the compressor frequency with a strong positive relationship. This is consistent with the normal operation of compressors. When the compressor speed is increased, the mass flow rate and the electrical consumption also increase.

In this case, the values for the correlation coefficient and the partial correlation coefficient among $\dot{W}_c$ and f_c are 0.881 and 0.986. The difference between them is that the partial correlation coefficient measures the dependence between the response and one independent variable, when the effect of the other independent variables is removed. Therefore, it is a better statistical indicator when we have so many independent variables, removing the interaction effect between them. As we can see in the correlation matrix above, the value of the partial correlation coefficient always indicates a stronger dependence compared to the correlation coefficient in all the relationships between the response and independent variables. As we will soon see, this value of 0.986 between $\dot{W}_c$ and f_c will allow us to transform the response and simplify the model construction.

The second main independent variable is T_{co} which also has a strong positive relationship with the compressor consumption ($pccp = 0.948$). Once again, this result is to be expected, due to the fact that the compressor installed in the DSHP is a scroll compressor. As has been reported in [10], when the frequency remains constant, the electrical consumption in scroll compressors is mainly fixed by the condensation temperature (or condensation pressure). Now, if we set the boundary conditions in the condenser, selecting the independent variables in the

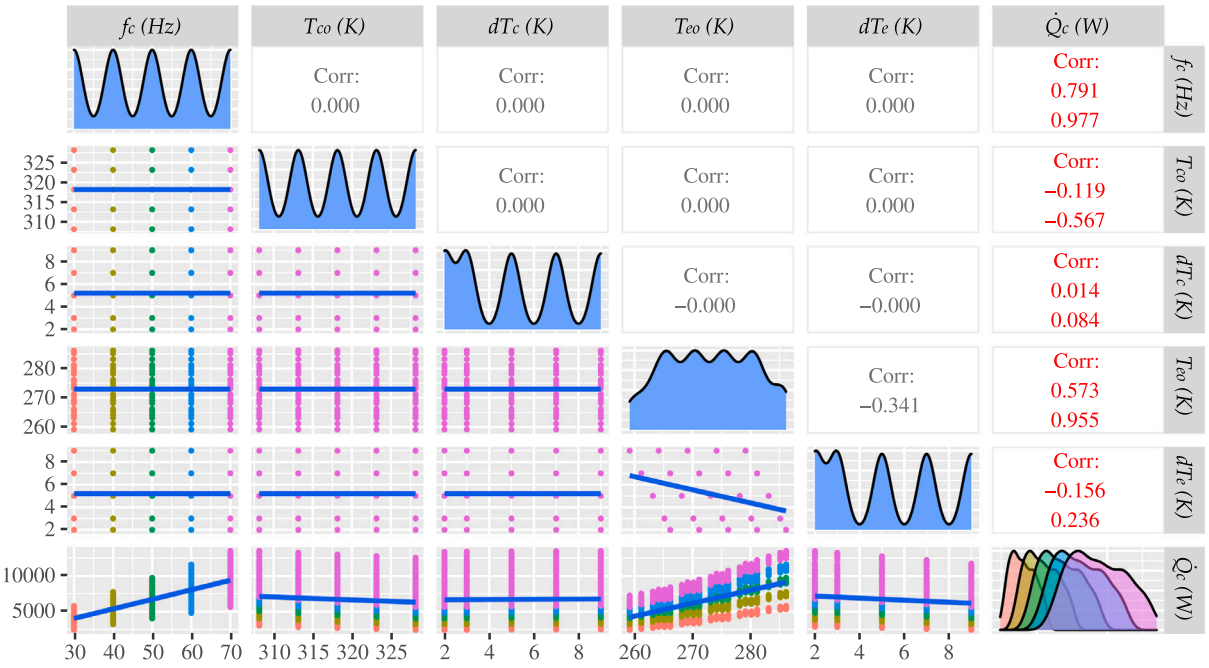

Fig. 8. WG: Correlation matrix $\dot{Q}_c$.

secondary loop, this dependence will be reproduced mainly by T_{co} and, to a lesser extent, dT_c. In this case, the $pccp$ of dT_c is −0.345 with a slight negative dependence. When the value of dT_c is increased, the mass flow rate in the secondary loop of the condenser decreases. So, for a given supply temperature to the building, we have a slight reduction in the condensation temperature and pressure ratio, a slight rise in the compressor efficiency, and therefore a small reduction in $\dot{W}_c$.

Then, regarding the independent variables relating to the evaporator, we have a positive relationship between $\dot{W}_c$ and T_{eo} ($pccp = 0.492$, a secondary dependence compared to f_c and T_{co}), and a null or really small effect with dT_e ($pccp = 0.04$). The effect of the evaporation temperature/pressure on $\dot{W}_c$ was also analyzed in [10] for a large number of scroll compressors, and it presented a positive (low range of evaporation pressure) or negative relationship (middle range of evaporation pressure). In this case, we obtained similar results for the relationship between $\dot{W}_c$ and T_{eo}: a positive relationship in the WG mode (low range of P_e) and a negative relationship in SG mode with a $pccp = -0.596$ (middle range of P_e).

From the discussion above we can say that, in WG mode, the compressor consumption is mainly fixed by f_c and T_{co} with a strong positive relationship. Then, we have a secondary positive dependence with T_{eo} and small dependencies with dT_c (negative) and dT_e (really small and slight positive).

These results can also be observed in the scatter plots of the correlation matrix. Of course, having so many independent variables makes identifying the relationships a complicated process. The clearest dependencies can be seen for the main variables f_c and then T_{co}. As mentioned above, the first one shows a clear positive dependence and, by selecting a specific level of frequency, we can observe a vertical deviation due to the effect of the other independent variables. This deviation is even greater as f_c increases, and it is confirmed by the density plot of $\dot{W}_c$ (The range on the x-axis of the density plot, the right lower corner plot, increases at higher compressor frequencies). Therefore, if we construct a polynomial model to correlate $\dot{W}_c$, we will need to consider some interaction terms with f_c. Then, the scatter plot of T_{co} shows the same positive dependence with a high degree of vertical deviation. In this case, thanks to the color series, we can identify that this vertical deviation is mostly caused by f_c.

Now, making the same analysis on $\dot{Q}_c$ and $\dot{Q}_e$, Figs. 8 and 9 shows the correlation matrices for the capacities.

According to the calculated values of the $pccp$, the order from the most important variables (strong dependence) to secondary variables (slight dependence) is:

- $\dot{Q}_c \Rightarrow f_c$ (0.977), T_{eo} (0.955), T_{co}(−0.567), dT_e (0.236) and dT_c (0.084).
- $\dot{Q}_e \Rightarrow f_c$ (0.963), T_{eo} (0.951), T_{co}(−0.752), dT_e (0.228) and dT_c (0.138).

Therefore, the main independent variable is still f_c with the same strong positive relationship. We have always obtained the same results for all the response variables ($\dot{W}_c$, $\dot{Q}_c$ and $\dot{Q}_e$) in the 7 operating modes. However, for the capacities, the other main independent variable is T_{eo} rather than T_{co}. In this case, as has been reported in [10], the mass flow rate in scroll compressors is mainly fixed by the evaporation temperature for a given compressor speed, and therefore T_{eo} is now the second main relationship concerning the capacities and, to a lesser extend dT_e.

Then, as concerns the condenser, T_{co} presents a negative dependence and dT_c a slight positive dependence.

On the one hand, when we have high values of hot water production, the condensation temperature is also higher; therefore for a fixed value of evaporation temperature, the pressure ratio increase and the volumetric efficiency on the compressor is decreased, with a negative effect on the capacities. On the other hand, as mentioned above, when dT_c is increased, the mass flow rate in the secondary loop of the condenser decreases. So, we have a slight reduction in the condensation temperature, a slight rise in the volumetric efficiency, and therefore a small rise in the capacities.

Once a preliminary analysis of the relationships between the response and the independent variables has been concluded, the second step is to find a suitable polynomial model to reproduce them.

In this sense, the first model to test would be a simple linear model including all the independent variables. This is the simplest model that we can build, and it should always be the first step when we construct a response surface model. Firstly selecting $\dot{W}_c$ to construct a response surface model, Fig. 10 and Table 5 on the left side show the results for the linear model. Moreover, they include the results of a second model (stepwise model) that uses automatic term selection tools to simplify

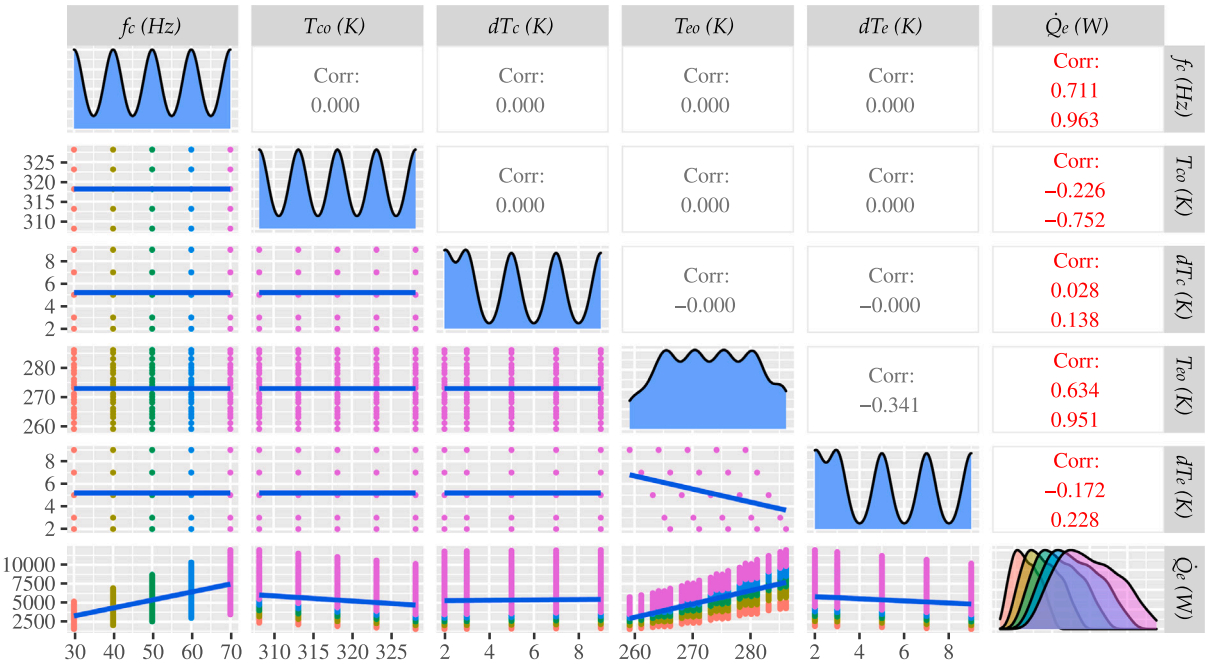

Fig. 9. WG: Correlation matrix $\dot{Q}_e$.

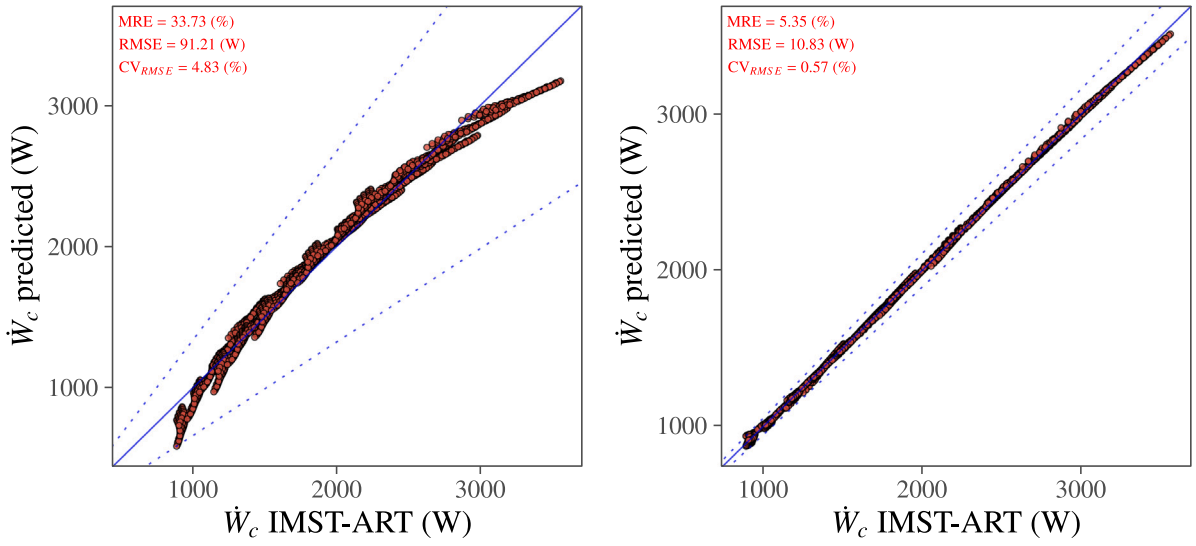

Fig. 10. WG: Linear model and stepwise model.

the comparison between these two models. This second model will be introduced later, when we finish analyzing the simple linear model.

Analyzing the results, we can establish that this first model, the linear model, with so few terms is not able to predict $\dot{W}_c$ with good accuracy. The graph predicted vs. experimental (Fig. 10-left) shows high values for MRE, RMSE and CV_{RMSE}. In addition, we can see how the represented points describe a parabola, which is indicative that there are some non-linear relationships not explained by the model. The latter can also be checked in the model's diagnostic plots (Fig. 11).

The residuals vs. fitted plot also shows a parabolic dependence, indicating that the residuals are not uncorrelated due to the unexplained relationships. Furthermore, the normal q-q plot indicates that the residuals do not have a normal distribution. Hence, we need to add more terms to the polynomial model in order to explain these relationships.

Regarding the steps to add terms in a polynomial model, there are different approaches which can be used.

For example, it is possible to construct the model adding terms until the added term is not statistically significant (forward regression). This statistical significance is measured by the *p-value* considering that a predictor should be included in the model when it has a *p-value* < 0.05. Table 5 also includes the *p-value* of the predictors adding significance stars to the calculated regression coefficients.

Then, the other option is to use the reverse method (backward regression). In this case, we select a specific polynomial degree including all the predictors in the model (linear terms, interaction terms, etc.). Then, the predictors with highest *p-value* are removed iteratively until only significant predictors remain.

In both cases, we get compact polynomial models able to predict the response variable with a low deviation. It is important to note that lower order terms should not be removed from the model before higher order terms in the same independent variable, even if it shows a non significant *p-value* [see 45, pg. 130-131].

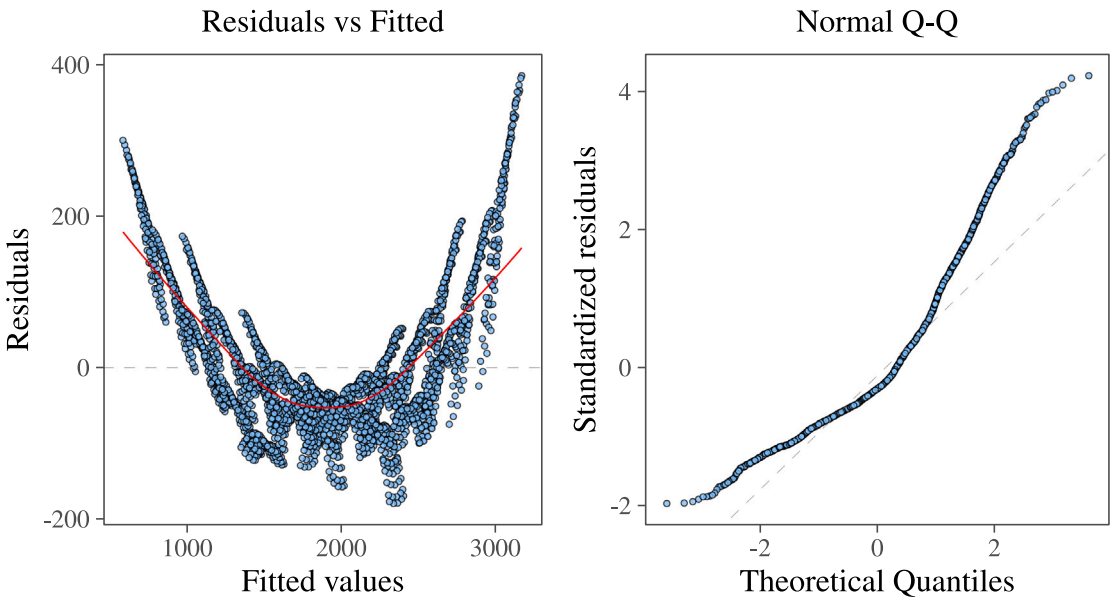

Fig. 11. WG: Linear model diagnostic plots.

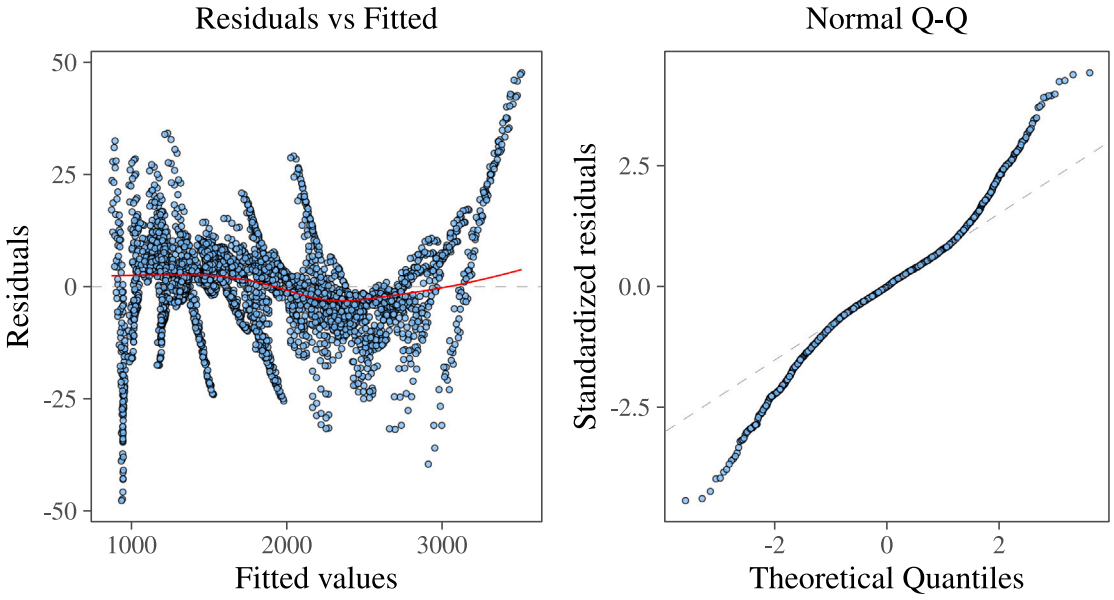

Fig. 12. WG: Stepwise model diagnostic plots.

It is likely that the methods described above are useful in many applications and provide us with a simple way to construct accurate polynomial models. However, when we have a significant number of independent variables, these methodologies become unwieldy.

In order to simplify the model construction when a significant number of independent variables are involved in the modeled process, a third option is to use the stepwise regression. In this case, the model construction is carried out by an automatic procedure. This method combines backward elimination and forward selection in a criterion-based procedure.

Selecting this third option applied to a second-order polynomial model and considering the Akaike (AIC) criterion, the stepwise regression procedure obtains the model provided in Fig. 10 and Table 5 on the right side. The *stepAIC()* R function [see 46, pg. 143] has been used to facilitate the application of the stepwise regression procedure.

Let us now consider the results for this second model. We can see that the values of MRE and RMSE have decreased significantly. Moreover, Fig. 12 shows a lower scale in the residuals with low grouping patterns and all the regression coefficients included in Table 5 are statistically significant.

Regarding these regression coefficients, we can compare them with the coefficients obtained at the beginning in the adjustment of the first model. If we look at the sign of each of the coefficients in the simple linear model, we can see that they correspond to the sign obtained in the calculation of the partial correlation coefficients of Pearson (Fig. 7). On the other hand, the second model proposed does not keep this equality. This is completely normal due to a greater number of predictors having been introduced, which may include interaction terms and quadratic terms for the same independent variable. This means that the effect of an independent variable on the response variable is divided into several terms of the model.

However, if we take a look at the total number of terms included in the second model, we will notice that the stepwise methodology has only eliminated one term ($dT_c \times dT_e$), with a total of 20 regression coefficients. It is possible that some terms provide little information despite

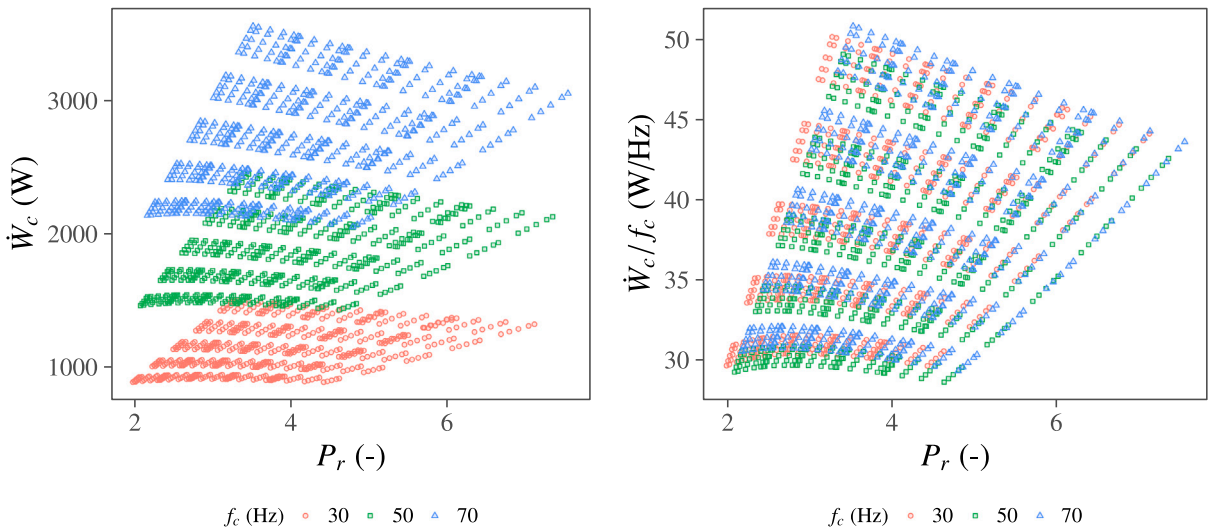

Fig. 13. WG: $\dot{W}_c$ and $\dot{W}_c/f_c$ vs. pressure ratio.

Table 5
WG: Linear model and stepwise model coefficients.

	$\dot{W}_c$ (W) (linear model)	$\dot{W}_c$ (W) (stepwise regression model)
(*Int.*)	−1.413e+04 (±1.92e+02)***	7.096e+04 (±1.35e+03)***
f_c	3.850e+01 (±2.26e−01)***	−2.704e+02 (±1.63e+00)***
T_{co}	3.825e+01 (±4.53e−01)***	−3.918e+02 (±6.18e+00)***
dT_c	−1.310e+01 (±1.25e+00)***	1.834e+02 (±8.66e+00)***
T_{eo}	7.286e+00 (±4.53e−01)***	−6.209e+01 (±5.62e+00)***
dT_e	1.500e+00 (±1.33e+00)*	−1.498e+01 (±1.06e+01)**
(f_c^2)		1.461e−01 (±2.28e−03)***
(T_{co}^2)		3.798e−01 (±9.11e−03)***
(dT_c^2)		4.150e−01 (±7.68e−02)***
(T_{eo}^2)		−2.150e−01 (±9.11e−03)***
(dT_e^2)		−1.318e−01 (±8.02e−02)**
$f_c \times T_{co}$		7.586e−01 (±3.81e−03)***
$f_c \times dT_c$		−2.919e−01 (±1.05e−02)***
$f_c \times T_{eo}$		1.989e−01 (±3.81e−03)***
$f_c \times dT_e$		3.437e−02 (±1.12e−02)***
$T_{co} \times dT_c$		−5.157e−01 (±2.10e−02)***
$T_{co} \times T_{eo}$		5.586e−01 (±7.62e−03)***
$T_{co} \times dT_e$		1.297e−01 (±2.24e−02)***
$dT_c \times T_{eo}$		−8.192e−02 (±1.98e−02)***
$T_{eo} \times dT_e$		−9.163e−02 (±2.78e−02)***
Num.Obs.	3125	3125
R2 Adj.	0.978	1.000
AIC	37 089.8	23 799.3
MRE (%)	33.735	5.354
RMSE (W)	91.212	10.829
CV_{RMSE} (%)	4.835	0.574
Range (W)	[890, 3558]	[890, 3558]

[a] + p < 0.1, * p < 0.05, ** p < 0.01, *** p < 0.001.
[b] Temperatures (K).
[c] Compressor frequency (Hz).

being statistically significant and the model can be further compacted, but with a total of 20 coefficients the model obtains approximately 5% of MRE. Removing terms will increase this error.

In this sense, applying a transformation in the response variable can simplify the model construction and improve the prediction results. This is a common technique used in regression models. For example, the Box–Cox power transformation is commonly applied when models violate the normality assumption [see 47, pg. 199-200]. Another possibility is to carry out a transformation using the independent variables. For this purpose, we need to know and understand the physical process modeled.

From the results obtained in the correlation matrices, we could see that the most relevant independent variable is f_c when we characterize the compressor consumption and also the capacities, with a strong positive dependence. Mainly, the compressor speed will fix the refrigerant mass flow rate in the primary loop and hence the electrical consumption in the compressor and the capacities. From the equations to calculate the compressor efficiency and the volumetric efficiency, Eqs. (22)–(24) show how to remove the main dependence of the compressor speed in the unit performance:

$$\dot{W}_c = \frac{\dot{m}_{ref}\,\Delta h_{is}}{\eta_c} \Rightarrow \dot{W}_c = \rho_s\, n\, V_s\, \frac{\eta_v}{\eta_c}\, \Delta h_{is} \Rightarrow \boxed{\frac{\dot{W}_c}{n} = \rho_s\, V_s\, \Delta h_{is}\, \frac{\eta_v}{\eta_c}} \tag{22}$$

$$\dot{Q}_c = \dot{m}_{ref}\,\Delta h_{23} \Rightarrow \dot{Q}_c = \rho_s\, n\, V_s\, \eta_v\, \Delta h_{23} \Rightarrow \boxed{\frac{\dot{Q}_c}{n} = \rho_s\, V_s\, \eta_v\, \Delta h_{23}} \tag{23}$$

$$\dot{Q}_e = \dot{m}_{ref}\,\Delta h_{13} \Rightarrow \dot{Q}_e = \rho_s\, n\, V_s\, \eta_v\, \Delta h_{13} \Rightarrow \boxed{\frac{\dot{Q}_e}{n} = \rho_s\, V_s\, \eta_v\, \Delta h_{13}} \tag{24}$$

Therefore, a possible transformation to apply could be to divide the response variables by f_c, so we obtain $\dot{W}_c/f_c$, $\dot{Q}_c/f_c$, and $\dot{Q}_e/f_c$ as new response variables. Fig. 13 shows the effect when we apply this transformation, plotting $\dot{W}_c$ and $\dot{W}_c/f_c$ as a function of the pressure ratio. Clearly, the major effects of f_c are removed from the response variable $\dot{W}_c/f_c$. The figure on the left side shows different groups or levels for the electrical consumption depending on the compressor speed but, once the transformation is applied, the figure on the right side shows how these levels converge in a single group with only a slight dependence of the compressor speed.

At this time, it is important to keep in mind that, when a transformation is applied, the interpretations must be based on the transformed variables, not on the original variables. Thus, it is recommended to regenerate the correlation matrices and recheck the dependencies of the new response variables with the independent variables. Figs. 14–16 are the correlation matrices generated for the new response variables.

If we look at the correlation matrices included above, we will also see that the dependence on the compressor frequency has been practically removed. Then, regarding the values of the *pccp*, we can see that they increase for the rest of the independent variables, maintaining the same sign. Therefore, the rest of the dependencies continue to maintain the same trend with a greater significance.

Let us now include a final response surface model for the characterization of $\dot{W}_c/f_c$ rather than $\dot{W}_c$. In order to build it, the stepwise

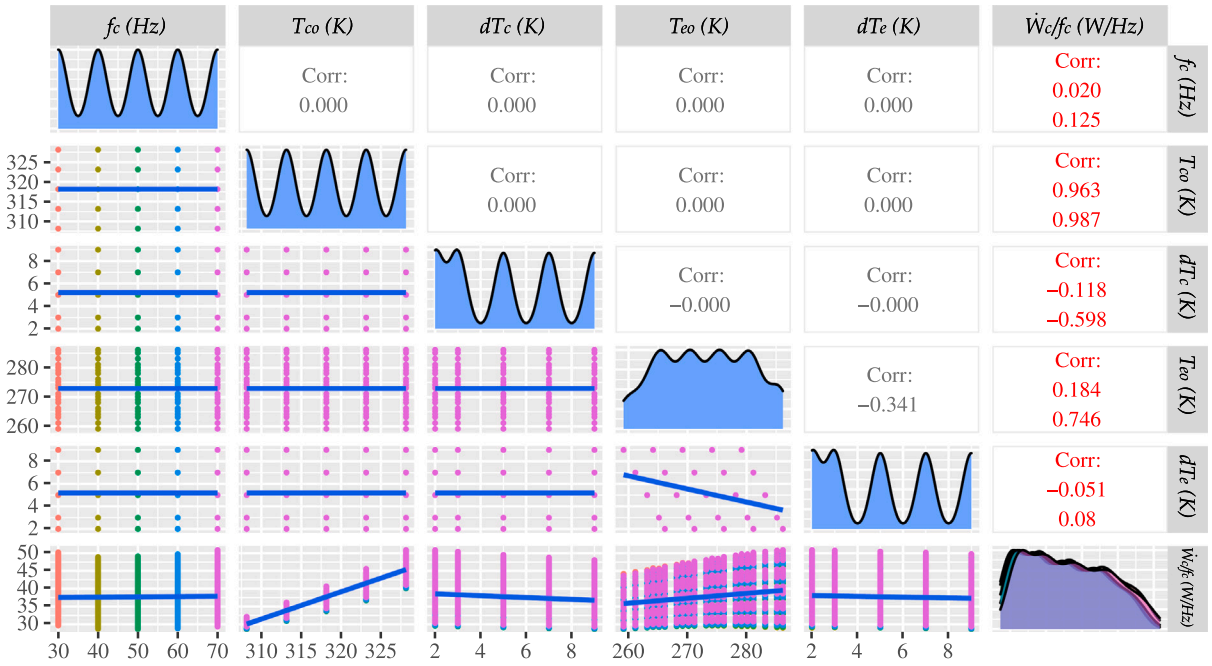

Fig. 14. WG: Correlation matrix $\dot{W}_c/f_c$.

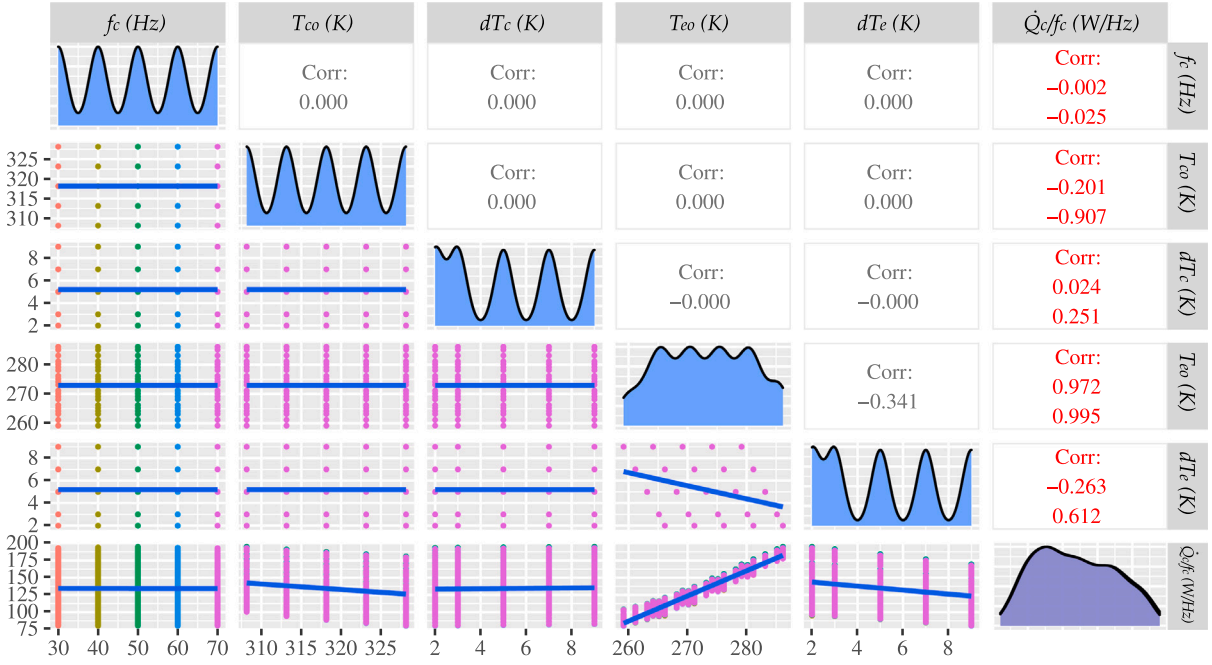

Fig. 15. WG: Correlation matrix $\dot{Q}_c/f_c$.

regression method was applied considering a second-order polynomial with a greater penalty in the terms of inclusion. The objective was to include only the most relevant terms to obtain a compact polynomial model without distribution patterns in the residuals plot. The independent variable f_c is also included in order to reproduce the second-order dependencies that the transformation has not eliminated. Moreover, an extra term $(1/f_c)$ was also included to decrease the error prediction. This coefficient corresponds to an interception term when we recalculate $\dot{W}_c$ from $\dot{W}_c/f_c$. Table 6, Figs. 17 and 18 include the results for this last model.

As can be seen in the results included above, this last model improves the results of the second model adjusted with a significant reduction in the number of regression coefficients, with an MRE of less than 2%. The values of MRE, RMSE and CV_{RMSE} have been recalculated for the compressor consumption rather than $\dot{W}_c/f_c$ in order to compare the results with the previous models adjusted. Moreover, Fig. 18 on the left side shows a lower scale in the residuals without grouping patterns and the residuals have a normal distribution (Fig. 18-right). These residuals have also been recalculated as values for the compressor consumption.

Therefore, due to the fact that this last model has a lower prediction error with only 12 coefficients, it has been selected as the final model for the characterization of the compressor energy consumption in Winter Ground. Regarding the capacities, if we apply the same steps described above, we will obtain the same polynomial model but with the interaction term $T_{co} \times dT_c$ removed as a non significant term. These

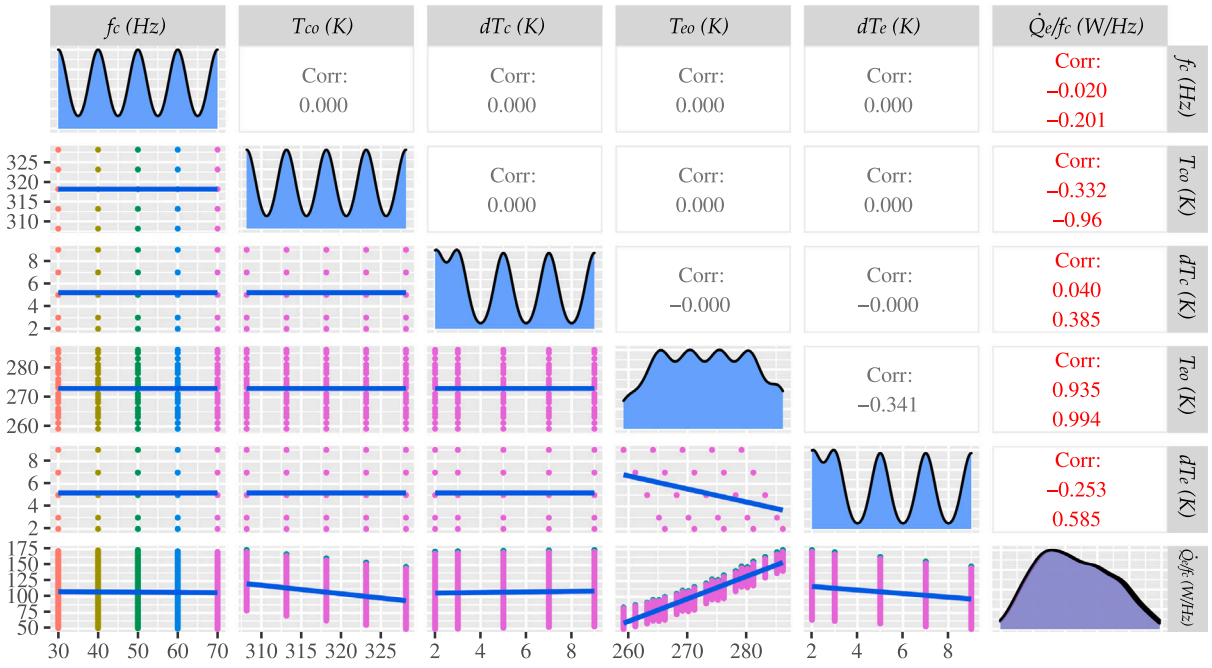

Fig. 16. WG: Correlation matrix $\dot{Q}_e/f_c$.

Table 6
WG: $\dot{W}_c/f_c$ model.

	$\dot{W}_c/f_c$ (W/Hz)
(*Int.*)	1.162e+03 (±1.35e+01)***
(T_{co}^2)	7.612e−03 (±1.00e−04)***
T_{co}	−6.997e+00 (±6.74e−02)***
(T_{eo}^2)	−3.968e−03 (±7.56e−05)***
T_{eo}	−1.214e+00 (±4.83e−02)***
dT_c	3.013e+00 (±7.38e−02)***
dT_e	3.174e−02 (±1.74e−03)***
f_c	−1.602e−01 (±1.08e−02)***
$(1/f_c)$	2.991e+02 (±2.53e+00)***
$T_{co} \times T_{eo}$	1.089e−02 (±7.90e−05)***
$T_{co} \times dT_c$	−1.029e−02 (±2.32e−04)***
$T_{eo} \times f_c$	1.125e−03 (±3.95e−05)***
Num.Obs.	3125
R2 Adj.	1.000
AIC	−4384.6
MRE (%)	1.385
RMSE (W)	5.524
CV_{RMSE} (%)	0.293
Range (W)	[890, 3558]

[a] + p < 0.1, * p < 0.05, ** p < 0.01, *** p < 0.001.
[b] Temperatures (K).
[c] Compressor frequency (Hz).

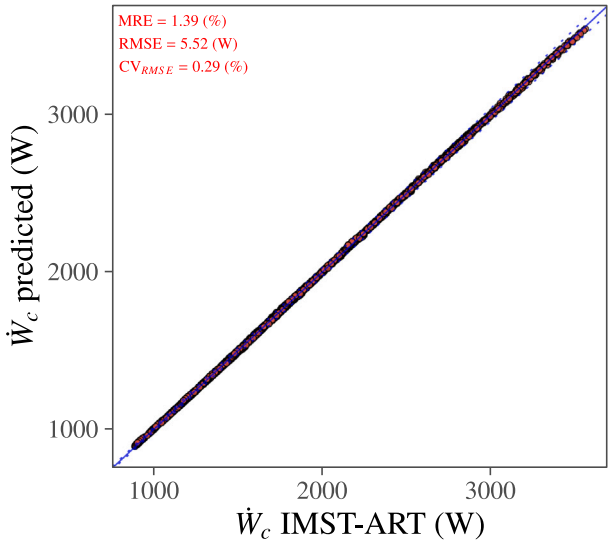

Fig. 17. WG: $\dot{W}_c/f_c$ model.

results are summarized in supplementary material, together with the models obtained for the rest of the operating modes.

5.4. Winter air polynomial models

In order to not extend the explanation, this subsection only includes some special aspects to consider when we characterize an aerothermal unit. This mainly relates to how to include the dehumidification effect in the unit performance when the RTPFHx works as an evaporator.

This effect does not influence the characterization of the compressor consumption, but it must be included in the characterization of the capacities. It directly affects the evaporator capacity, increasing its value due to the extra latent capacity when dehumidification conditions are present. Then, this rise in the evaporator capacity will also modify the value of the condenser capacity ($\dot{Q}_c = \dot{Q}_e + \xi \dot{W}_c$).

As in Winter Ground mode, the response variables characterized have been $\dot{W}_c/f_c$, $\dot{Q}_c/f_c$ and $\dot{Q}_e/f_c$ and the polynomial models have been obtained considering a second-order polynomial and the stepwise methodology. The independent variables to include are f_c, T_{ei}, f_{fan}, T_{co}, dT_c and the humidity conditions fixed by RH. Additionally, during the model construction, it was found that applying a transformation over the predictor f_{fan} and considering $1/f_{fan}$ as an independent variable improved the results. Then, the extra term $1/f_c$, considered in Winter Ground, is also included.

Regarding the humidity conditions in the evaporator, the boundary variable is the air relative humidity (RH) at the inlet of the RTPFHx

At the beginning, this variable was considered in the model's construction in order to introduce the dehumidification effect. However, directly considering RH as a predictor only slightly improved the results, and the analysis of the residuals continued to show effects not explained by the model.

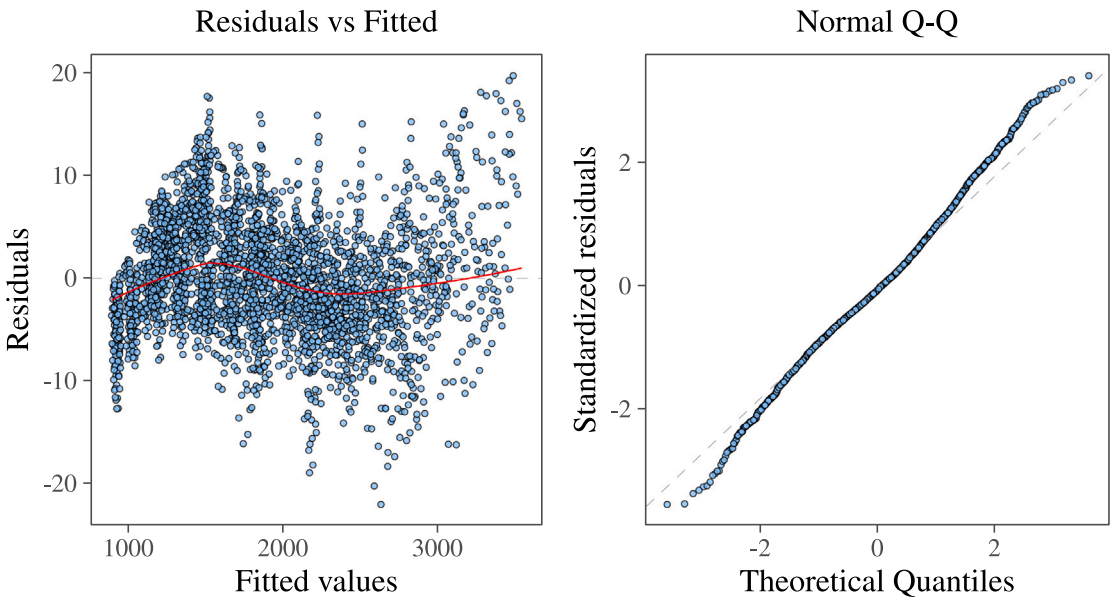

Fig. 18. WG: $\dot{W}_c/f_c$ model diagnostic plot.

This was an expected value due to the fact that the dehumidification process in the RTPFHx occurs only when the external wall surfaces of the round tubes are below the corresponding dew point temperatures, but:

1. *"How can we reproduce the dehumidification effect in a polynomial model?"*
2. *"Which is the independent variable to include when the external variables are the only input information?"*

Clearly, the independent variable selected must be able to increase the capacity value taking into account the latent heat under dehumidification conditions. On the other hand, this term should not modify the value of the capacity when there is no condensation in the RTPFHx.

The solution adopted was to estimate the difference between the air inlet humidity ratio (w_{ai}) and the air humidity ratio considering an air temperature equal to the evaporation temperature (w_{sat}), because the temperature in the external wall surfaces of the round tubes is expected to be close to the evaporation temperature. This means that we will need to include the air inlet temperature, the relative humidity and some estimation for the evaporation temperature as input information. This estimation of the evaporation temperature will be necessary to build the polynomial models taking just the external variables into account as available information.

Therefore, in order to estimate the evaporation temperature, a constant temperature approach has been considered. For Winter Air mode, this temperature approach is calculated as the mean of the values obtained in the virtual database, i.e. $\delta T_e = 6\,K$. Then, the evaporation temperature and the difference in the humidity ratio are estimated as:

$$T_e \approx T_{ai} - \delta T_e \tag{25}$$

$$\Delta w = w_{ai}(T_{ai}, RH, P_{atm}) - w_{sat}(T_{ai} - \delta T_e, P_{atm}) \tag{26}$$

The values calculated with the equation above can be positive or negative. If the calculated value is positive, we will have condensation in the RTPFHx. Therefore, in order to reproduce the dehumidification process adequately, we must to recalculate Δw as:

$$\Delta w' = \max\left[w_{ai}(T_{ai}, RH, P_{atm}) - w_{sat}(T_{ai} - \delta T_e, P_{atm}), 0\right] \tag{27}$$

Therefore, the $\Delta w'$ calculated with Eq. (27) provides us with an independent variable able to modify the capacity value only when we have dehumidification conditions in the RTPFHx. The only requirement will be to estimate $\Delta w'$ as is described above using a psychrometric chart or any software able to obtain the psychrometric properties of the humid air. In order to calculate these properties, the *HAPropsSI()* function available in the Coolprop [48] software has been used.

Finally, the polynomial models adjusted for Winter Air mode include $\Delta w'(T_{ai}, RH, \delta T_e, P_{atm})$ and f_c, T_{ei}, f_{fan}, T_{co}, dT_c as independent variables. These models are also summarized in the supplementary material.

6. Summary of results

Once the procedure followed to obtain the polynomial models from the analysis of the virtual database has been described, this section includes a summary of results. Three polynomial equations were obtained for each operating mode to predict the compressor energy consumption and evaporator and condenser capacities. Therefore, considering the seven operating modes, a total of 21 polynomial models were fitted for characterizing the DSHP unit. These models have been fitted by regression adjustment using the data for each operating mode available in the virtual database. As previously mentioned, the analysis has been performed on a dual source heat pump in this study. Therefore, these polynomial models are suitable for characterizing aerothermal and geothermal heat pumps and chillers. They offer a simple way of describing the behavior of these units, allowing a straightforward prediction of their performance. Similarly, this technique is commonly used in refrigeration compressors, where the polynomials developed in this work allow considering these units as simple components that can be implemented in systems with a greater number of elements and complexity. Table 7 includes a summary of the prediction errors between the prediction of the polynomial models compared to the fitted data. A complete summary, including the value of the regression coefficients and comparative plots, is included in the supplementary material.

As can be seen, the results predicted by the developed polynomial models are in very good agreement with the simulated results generated with the DSHP detailed model (<5% of MRE and most cases <2% with a $CV_{RMSE} < 1\%$). It is essential to emphasize that within the simulations generated by IMST-ART, every operating mode incorporates the full working map. Therefore, selecting all the simulated results as training points allows us to obtain accurate polynomial models and remove possible extrapolation errors.

Table 7
Prediction errors for the final polynomial models.

	$\dot{W}_c$	$\dot{Q}_c$	$\dot{Q}_e$
Winter Ground			
MRE (%)	1.385	1.867	3.204
RMSE (W)	5.524	32.030	31.981
CV_{RMSE} (%)	0.293	0.477	0.596
Summer Ground			
MRE (%)	1.269	1.141	1.286
RMSE (W)	3.578	38.031	38.663
CV_{RMSE} (%)	0.287	0.373	0.417
DHW Ground			
MRE (%)	1.506	4.259	7.834
RMSE (W)	8.963	50.027	56.302
CV_{RMSE} (%)	0.411	0.658	0.929
DHW User			
MRE (%)	1.150	1.458	2.587
RMSE (W)	7.123	39.704	49.260
CV_{RMSE} (%)	0.313	0.432	0.655
Winter Air			
MRE (%)	1.806	2.465	2.891
RMSE (W)	6.319	58.656	51.994
CV_{RMSE} (%)	0.333	0.720	0.766
Summer Air			
MRE (%)	3.355	1.477	1.894
RMSE (W)	8.381	36.179	35.344
CV_{RMSE} (%)	0.534	0.375	0.417
DHW Air			
MRE (%)	1.383	2.648	3.878
RMSE (W)	9.953	57.066	60.869
CV_{RMSE} (%)	0.448	0.626	0.808

7. Conclusions

This paper presents a detailed analysis of how to model geothermal and aerothermal heat pumps and chillers using empirical models capable of accurately predicting the unit's performance for the entire working map. The following main conclusions have been obtained:

- The new prototype of DSHP analyzed in this work operates with R32 refrigerant and includes a variable speed compressor which gives full capabilities for efficient modulating operation. The unit can select a total of 7 operating modes by selecting between heat pump or chiller operation and allowing the use of geothermal and aerothermal loops as sources. Therefore, considering the same unit, this work shows how to obtain a suitable characterization by using empirical models for the main heat pump and chillers technologies available in the market.
- The performance of current vapor compression heat pump and refrigeration units with variable speed components has, in general, 5 independent variables, for instance: inlet and outlet temperature of the secondary flow at the evaporator and the condenser, plus the compressor frequency. Therefore, the response surface for the evaporator capacity, condenser capacity, and energy consumption lies on a 5D domain.
- A substantial number of test points would be necessary to conduct an experimental campaign using a full factorial test plan, such as 3125 points when considering 5 levels for each independent variable. For the detailed analysis of the performance response surfaces of the unit, a dataset of virtual experiments was generated using a detailed model developed in the commercial software IMST-ART. The detailed model can predict the unit performance with an error of less than 10%. The performance maps generated for the 7 operating modes include a total of 21875 simulation points.
- Simulations using a detailed model of the unit have proven to be effective in generating the unit performance maps. This approach has allowed the subsequent analysis of the simulations in order to establish the most appropriate polynomial expressions. Furthermore, this approach can be combined with the generation of experimental results with which, once the simulation results fix the polynomial expressions, they can be readjusted to experimental data, thus increasing the accuracy of the models.
- The results show that the unit's performance can be characterized very efficiently by adequate polynomials. The analysis of the virtual database has obtained these polynomials. This analysis found that the polynomials include a smaller number of terms if we select the energy consumption and capacities divided by compressor speed as response variables. The independent variables selected to perform the polynomial models are the external variables. Therefore, the models generated in this work characterize the unit as a single component and can be easily implemented in more complex system models with a larger number of components.

This study generally shows how to build polynomial models to characterize current heat pump units and chiller with variable speed components. The selected approach demonstrated to obtain satisfactory results for modeling systems with a large number of independent variables. Considering the unit as a single component provides these models with great flexibility, allowing the engineer or researcher to implement them while developing models that include more complex systems with larger components. The polynomial equations developed have been obtained from an exhaustive analysis of many simulation data for different heat pump technologies. These equations can be used to model other units only requiring a minimum number of training data to rescale the corresponding regression coefficients. Future investigations of this work are intended to analyze the minimum sample size needed and the most appropriate Design of Experimental methodology to optimize the acquisition of new training data in other units.

Declaration of competing interest

The authors declare that they have no known competing financial interests or personal relationships that could have appeared to influence the work reported in this paper.

Data availability

Data will be made available on request.

Acknowledgments

The present work has been supported by the European Community Horizon 2020 Program for European Research and Technological Development (2014–2020) inside the framework of the project 656889 – GEOTeCH (Geothermal Technology for Economic Cooling and Heating), by the project "DESCARBONIZACIÓN DE EDIFICIOS E INDUSTRIAS CON SISTEMAS HÍBRIDOS DE BOMBA DE CALOR", funded by the "Ministerio de Ciencia e Innovación", MCIN, Spain, with code number: PID2020-115665RB-I00 and by the "Ministerio de Educación, Cultura y Derporte", MECD, Spain, inside the program "Formación de Profesorado Universitario (FPU15/03476)". Many thanks as well to the late Dr. José Miguel Corberán, without whom this work would never have been possible. Sadly, Dr. José Miguel Corberán passed away in July of 2022. I wish to give my wholehearted support to José Miguel's family. I hope we did you proud.

Appendix A. Supplementary data

Supplementary material related to this article can be found online at https://doi.org/10.1016/j.applthermaleng.2023.121743.

References

[1] J.F. Hamilton, J. Miller, A simulation program for modeling an air conditioning system, in: Winter Meeting - Atlanta, GA, ASHRAE Transactions, 1990, Volume 96(1), pages 213–221.

[2] C. Fischer, S.K. Rice, ORNL Heat Pump Model: A Steady-State Computer Design Model of Air-to-Air Heat Pumps, Oak Ridge National Laboratory (ORNL), Oak Ridge, TN (United States), 1983, http://dx.doi.org/10.2172/814817, Fortran-IV computer program.

[3] J. Brown, R. Brignoli, P. Domanski, Y. Yoon, CYCLE_D-HX: NIST Vapor Compression Cycle Model Accounting for Refrigerant Thermodynamic and Transport Properties; Version 2, User's Guide, 2021, http://dx.doi.org/10.6028/NIST.TN.2134.

[4] D.H. Richardson, H. Jiang, D. Lindsay, R. Radermacher, Optimization of Vapor Compression Systems via Simulation, in: International Refrigeration and Air Conditioning Conference. Paper 529, Purdue University, West Lafayette, Indiana, 2002.

[5] D.H. Richardson, An Object Oriented Simulation Framework For Steady-State Analysis Of Vapor Compression Refrigeration Systems And Components (Ph.D. thesis), University of Maryland, 2006.

[6] H. Jiang, V. Aute, R. Radermacher, CoilDesigner: a general-purpose simulation and design tool for air-to-refrigerant heat exchangers, Int. J. Refrig. 29 (4) (2006) 601–610, http://dx.doi.org/10.1016/J.IJREFRIG.2005.09.019.

[7] J.M. Corberán, J. Gonzálvez, P. Montes, R. Blasco, 'ART' A Computer Code To Assist The Design Of Refrigeration and A/C Equipment, in: International Refrigeration and Air Conditioning Conference. Paper 570, Purdue University, West Lafayette, Indiana, 2002.

[8] T.A. IUIIE, IMST-ART: A simulation tool to assist the selection, design and optimization of refrigeration equipments and components, IMST-GROUP, Instituto de Ingeniería Energética (Universitat Politècnica de València), Camino de Vera S/N, 46022, Valencia (Spain), 2019, Version 3.9.

[9] AHRI 540, AHRI 540 - Standard for performance rating of positive displacement refrigerant compressors and compressor units, 2020.

[10] J. Marchante-Avellaneda, J.M. Corberán, E. Navarro-Peris, S.S. Shrestha, A critical analysis of the AHRI polynomials for scroll compressor characterization, Appl. Therm. Eng. 219 (2023) 119432, http://dx.doi.org/10.1016/J.APPLTHERMALENG.2022.119432.

[11] J. Marchante-Avellaneda, E. Navarro-Peris, J. Corberan, S.S. Shrestha, Analysis of map-based models for reciprocating compressors and optimum selection of rating points, Int. J. Refrig. 153 (2023) 168–183, http://dx.doi.org/10.1016/j.ijrefrig.2023.06.002.

[12] J.J. Allen, J.F. Hamilton, Steady-state reciprocating water chiller models, in: Annual Meeting - Washington DC, ASHRAE Transactions, 1983, Volume 89(2), pages 398–407.

[13] T. Afjei, R. Dott, Heat pump modelling for annual performance, design and new technologies, in: 12th Conference of International Building Performance Simulation Association, 2011, pp. 2431–2438.

[14] S.A. Tabatabaei, J. Treur, E. Waumans, Comparative evaluation of different computational models for air source heat pump based on real word data, in: Energy Procedia, vol. 95, Elsevier Ltd, 2016, pp. 459–466, http://dx.doi.org/10.1016/j.egypro.2016.09.065.

[15] T. Afjei, M. Wetter, A. Glass, TRNSYS type 204: Dual-stage compressor heat pump including frost and cycle losses, 1997, TRNSYS Type version 2.0.

[16] EnergyPlus Core Team, EnergyPlus: An open source building energy simulation program, 2022, Version 22.1.0. See Electric Chiller Model Based on Condenser Entering Temperature.

[17] J. Ruschenburg, T. Ćutić, S. Herkel, Validation of a black-box heat pump simulation model by means of field test results from five installations, Energy Build. 84 (2014) 506–515, http://dx.doi.org/10.1016/j.enbuild.2014.08.014.

[18] P. Pärisch, O. Mercker, J. Warmuth, R. Tepe, E. Bertram, G. Rockendorf, Investigations and model validation of a ground-coupled heat pump for the combination with solar collectors, Appl. Therm. Eng. 62 (2) (2014) 375–381, http://dx.doi.org/10.1016/J.APPLTHERMALENG.2013.09.016.

[19] S. Yuan, M. Grabon, Optimizing energy consumption of a water-loop variable-speed heat pump system, Appl. Therm. Eng. 31 (5) (2011) 894–901, http://dx.doi.org/10.1016/j.applthermaleng.2010.11.012.

[20] C. Verhelst, F. Logist, J. Van Impe, L. Helsen, Study of the optimal control problem formulation for modulating air-to-water heat pumps connected to a residential floor heating system, Energy Build. 45 (2012) 43–53, http://dx.doi.org/10.1016/j.enbuild.2011.10.015.

[21] H. Madani, J. Claesson, P. Lundqvist, Capacity control in ground source heat pump systems: Part I: Modeling and simulation, Int. J. Refrig. 34 (6) (2011) 1338–1347, http://dx.doi.org/10.1016/J.IJREFRIG.2011.05.007.

[22] H. Madani, J. Claesson, P. Lundqvist, Capacity control in ground source heat pump systems part II: Comparative analysis between on/off controlled and variable capacity systems, Int. J. Refrig. 34 (8) (2011) 1934–1942, http://dx.doi.org/10.1016/J.IJREFRIG.2011.05.012.

[23] A. Cazorla-Marín, J.M. Corberán, J. Marchante-Avellaneda, C. Montagud-Montalvá, Dual source heat pump, a high efficiency and cost-effective alternative for heating, cooling and DHW production, Int. J. Low-Carbon Technol. 13 (2) (2018) 161–176, http://dx.doi.org/10.1093/ijlct/cty008.

[24] A. Cazorla-Marín, C. Montagud-Montalvá, J.M. Corberán, J. Marchante-Avellaneda, Seasonal performance assessment of a dual source heat pump system for heating, cooling and domestic hot water production, in: International Ground Source Heat Pump Association Research Conference, IGSHPA, Stockholm, 2018, pp. 180–189, http://dx.doi.org/10.22488/okstate.18.000014.

[25] A. Cazorla Marín, Modelling and Experimental Validation of an Innovative Coaxial Helical Borehole Heat Exchanger for a Dual Source Heat Pump System (Ph.D. thesis), Universitat Politècnica de València, 2019, http://dx.doi.org/10.4995/THESIS/10251/125696.

[26] Y. Song, D. Rolando, J. Marchante Avellaneda, G. Zucker, H. Madani, Data-driven soft sensors targeting heat pump systems, Energy Convers. Manage. 279 (2023) 116769, http://dx.doi.org/10.1016/j.enconman.2023.116769.

[27] J.M. Cho, J. Heo, W.V. Payne, P.A. Domanski, Normalized performance parameters for a residential heat pump in the cooling mode with single faults imposed, Appl. Therm. Eng. 67 (1–2) (2014) 1–15, http://dx.doi.org/10.1016/j.applthermaleng.2014.03.010.

[28] M. Kim, W.V. Payne, P.A. Domanski, NISTIR 7350: Performance of a residential heat pump operating in the cooling mode with single faults imposed, in: NIST Interagency/Internal Report (NISTIR), Tech. rep., National Institute of Standards and Technology, Gaithersburg, MD, 2006.

[29] M. Kim, W.V. Payne, P.A. Domanski, S.H. Yoon, C.J. Hermes, Performance of a residential heat pump operating in the cooling mode with single faults imposed, Appl. Therm. Eng. 29 (4) (2009) 770–778, http://dx.doi.org/10.1016/j.applthermaleng.2008.04.009.

[30] M. Kim, S.H. Yoon, W.V. Payne, P.A. Domanski, Development of the reference model for a residential heat pump system for cooling mode fault detection and diagnosis, J. Mech. Sci. Technol. 24 (7) (2010) 1481–1489, http://dx.doi.org/10.1007/s12206-010-0408-2.

[31] J. Urchueguía, M. Zacarés, J. Corberán, A. Montero, J. Martos, H. Witte, Comparison between the energy performance of a ground coupled water to water heat pump system and an air to water heat pump system for heating and cooling in typical conditions of the European Mediterranean coast, Energy Convers. Manage. 49 (10) (2008) 2917–2923, http://dx.doi.org/10.1016/j.enconman.2008.03.001, URL https://linkinghub.elsevier.com/retrieve/pii/S0196890408000939.

[32] European Commission, Geothermal Technology for €conomic Cooling, 2015, *(H2020-LCE-2014-2, GEOTeCH-656889)*.

[33] HiRef, Hiref - Italian cooling solutions, 2020, Heat pumps manufacturer.

[34] J.M. Corberán, J. Marchante-Avellaneda, S. Martínez-Ballester, Deliverable D4.1. Dual source heat pump design, 2016, WP4 Plug&Play Geothermal System Development. GEOTeCH-656889.

[35] J.M. Corberan, C. Radulescu, J. Gonzálvez-Maciá, Performance Characterisation of a Reversible Water To Water Heat Pump, in: 9th International IEA Heat Pump Conference, Zürich, Switzerland, 2008, pp. 20–22, (May).

[36] J.M. Corberán, I. Martínez-Galván, S. Martínez-Ballester, J. Gonzálvez-Maciá, R. Royo-Pastor, Influence of the source and sink temperatures on the optimal refrigerant charge of a water-to-water heat pump, Int. J. Refrig. 34 (4) (2011) 881–892, http://dx.doi.org/10.1016/j.ijrefrig.2011.01.009.

[37] T. Xu, S. Sawalha, W. Mazzotti, B. Palm, Performance evaluation of a large capacity water-water heat pump using propane as refrigerant, in: 12th IIR Gustav Lorentzen Natural Working Fluids Conference, Edinburgh, UK, 2016, http://dx.doi.org/10.18462/iir.gl.2016.1129, (August).

[38] M. Pitarch, E. Navarro-Peris, J. Gonzálvez-Maciá, J.M. Corberán, Evaluation of different heat pump systems for sanitary hot water production using natural refrigerants, Appl. Energy 190 (2017) 911–919, http://dx.doi.org/10.1016/j.apenergy.2016.12.166.

[39] Grundfos, Grundfos sizing software, 2020, Online version.

[40] Wilo, Wilo-select 4 online, 2021, Online version.

[41] SWEP, SWEP calculation software, 2018, Version SSP G8.

[42] Copeland, Copeland select software, 2018, Version Select 8.

[43] S. Shao, W. Shi, X. Li, H. Chen, Performance representation of variable-speed compressor for inverter air conditioners based on experimental data, Int. J. Refrig. 27 (8) (2004) 805–815, http://dx.doi.org/10.1016/j.ijrefrig.2004.02.008.

[44] B. Standard, BS en 14511-3:2018. Air conditioners, liquid chilling packages and heat pumps for space heating and cooling and process chillers, with electrically driven compressors. Test methods, 2018.

[45] J.J. Faraway, Linear Models with R, CRC Press, Inc, New York, 2005.

[46] W.N. Venables, B.D. Ripley, MASS: Support functions and datasets for venables and ripley's MASS, 2022, URL https://cran.r-project.org/web/packages/MASS/index.html, R package version 7.3-55.

[47] R.I. Kabacoff, R in Action. Data Analysis and Graphics with R, second ed., Manning Publications Co., 2011.

[48] I.H. Bell, J. Wronski, S. Quoilin, V. Lemort, Pure and pseudo-pure fluid thermophysical property evaluation and the open-source thermophysical property library CoolProp, Ind. Eng. Chem. Res. 53 (6) (2014) 2498–2508, http://dx.doi.org/10.1021/ie4033999.